

BISTABILITY ANALYSIS OF AN APOPTOSIS MODEL
IN THE PRESENCE OF NITRIC OXIDE

by

Sercan Murat Şen

B.S. in Chemical Engineering, Boğaziçi University, 2007

Submitted to the Institute for Graduate Studies in
Science and Engineering in partial fulfillment of
the requirements for the degree of
Master of Science

Graduate Program in Chemical Engineering

Boğaziçi University

2009

dedicated to my family

ACKNOWLEDGMENTS

First of all, I would like to express my sincere thanks to my thesis supervisor Prof. Mehmet C. amurdan for his support and patience throughout my study. I wish to express my warm thanks to Dr. E. Zerrin Baęcı who has given continuous encouragement, clear-sighted suggestions and for introducing me to her research on apoptosis and relevant literature. It was also a privilege for me to work with her during the course of this thesis.

My sincere gratitude is due to my thesis committee members, Assist. Prof. Elif zkırmılı lmez and Assoc. Prof. Nesrin zren who devoted their valuable time to read and commented on my thesis.

Very special thanks to E. Nihal Korkmaz, Eralp Bolkent, Grkem Oęur, Sabriye Gven, İlker ztrk, Sadi T. Tezcanlı, (and other members of “Genlerbirlięi”), Pelin mit, Anda Armutlulu, Gray Kuzu, Seren Soner, Őlen Ekesan, Ilgaz Soykal and all my friends for their friendship and moral support which has given me strength.

I would like to thank to Zeynep Susam, Meri Ataman, Fatih Telis, Jeren Sahadova and Zeynep Canbek for their help in bistability analysis as a requirement of their senior projects. Cordial thanks for Belgin Balkan, Melike Grbz, Nurettin BektaŐ, Fatma Odak, Bilgi Dedeoęlu and Yakup Bal for their assistance and help.

I would like to acknowledge the Scientific and Technological Research Council of Turkey (TUBITAK) for the graduate scholarship during my M.S. studies.

Finally, I wish to thank my family for all their endless support, patience and encouragement throughout my life. Besides these, I would also express my great debt of gratitude to my family believing in me. This thesis is dedicated to them.

ABSTRACT

BISTABILITY ANALYSIS OF AN APOPTOSIS MODEL IN THE PRESENCE OF NITRIC OXIDE

Apoptosis, or programmed cell death, is a normal component of the development and healthy functioning of multicellular organisms. In apoptosis, cells die in response to a variety of stimuli in controlled and regulated ways. The apoptotic pathway is tightly regulated in the cell, since dysregulation of apoptosis may cause various illnesses. Decreased apoptosis induction is implicated in cancer (monostable cell survival) whereas increased apoptosis induction is implicated in neurodegenerative disorders (monostable cell death). In this study, the aim is to perform bistability analysis on the mitochondria-dependent apoptosis model under the influence of nitric oxide effects (NO) using Chemical Reaction Network (CRN) analysis. After obtaining ordinary differential equations derived from mass action kinetics, CRN analysis can be performed using a toolbox referred to as CRN Toolbox (CRNT). The model is decomposed into modules, since this toolbox can handle up to 20 complexes. Bistability in the modules is preserved throughout the whole model after the addition of other reactions in the pathway on these modules. Finally, two apoptotic and two cell survival states are obtained depending on the initial conditions in the cell. The results suggest that the anti-apoptotic effect of NO is responsible for the bistable character of the apoptotic pathway.

ÖZET

NİTRİK OKSİT İÇEREN APOPTOSİS MODELİNDE İKİ YÖNLÜ SEBATLILIK ANALİZİ

Apoptoz, ya da programlı hücre ölümü, çok hücreli canlıların gelişimlerinin ve sağlıklı fonksiyonlarının sağlanmasının bir parçasıdır. Programlı hücre ölümü sırasında hücreler birçok çeşit uyarıya karşılık olarak denetimli ve düzenlenmiş bir şekilde ölürlür. Programlı hücre ölümünün bozukluğu birçok hastalığa neden olduğundan, programlı hücre ölümü ağı hücre içerisinde sıkı bir şekilde düzenlenir. Programlı hücre ölümü oranında aşırı azalma (tek yönlü sebatlılık şeklinde hücrenin yaşamını sürdürmesi) kansere, programlı hücre ölümü oranında aşırı artış (tek yönlü sebatlılık şeklinde hücre ölümü) ise nörolojik hastalıklara sebebiyet verdiği bilinmektedir. Bu çalışmadaki amaç, nitrik oksit (NO) etkilerini içeren mitokondriye bağlı programlı hücre ölümü modeli üzerinde Kimyasal Tepkime Ağı analizi kullanarak iki yönlü sebatlılık analizi yapmaktır. Diferansiyel denklemlerin kütle etkisi kinetiğiyle çıkartılması sonucunda, Kimyasal Tepkime Ağı Araçutusu (CRNT) programı yardımıyla Kimyasal Tepkime Ağı (CRN) analizi gerçekleştirilebilir. Bu programın 20 kompleksle sınırlı olması nedeniyle model modüllere ayrıldı. Tepkime ağındaki diğer reaksiyonların bu modüller üzerine eklenmesi sonucunda modüller içerisinde elde edilen iki yönlü sebatlılık tüm model içerisinde korundu. Sonuç olarak, hücre içerisindeki başlangıç derişimlerine bağlı olan, ikisi apoptotik, ikisi ise hücrenin yaşamını sürdürdüğü durumlar elde edildi ve nitrik oksidin hücre ölümünü engelleyen etkisinin programlı hücre ölümü ağının iki yönlü sebatlılık niteliği göstermesine sebebiyet verdiği düşünüldü.

TABLE OF CONTENTS

ACKNOWLEDGMENTS	iv
ABSTRACT	v
ÖZET	vi
LIST OF FIGURES	ix
LIST OF TABLES	xiii
LIST OF SYMBOLS/ABBREVIATIONS	xvi
1. INTRODUCTION	1
2. THEORETICAL BACKGROUND AND SIGNIFICANCE	4
2.1. Apoptosis	4
2.2. FAS Mediated Apoptosis	7
2.3. Apoptosis Models	9
2.3.1. Bistability and Apoptosis	9
2.3.2. A Mitochondria-Dependent Apoptosis Model	10
2.3.3. Nitric Oxide Effects on the Mitochondria-Dependent Apoptosis Model	12
2.4. Chemical Reaction Network Theory	15
2.4.1. Reaction Networks and Their Structure	15
2.4.1.1. Complexes of a Network	15
2.4.1.2. The Reaction Vectors for a Network	16
2.4.1.3. The Stoichiometric Subspace for a Network	16
2.4.1.4. The Linkage Classes of a Network	17
2.4.1.5. Mass Action Kinetics	17
2.4.1.6. Weakly Reversible Networks	17
2.4.1.7. The Deficiency of a Network	17
2.4.1.8. The Deficiency Zero Theorem	18
2.4.1.9. The Deficiency One Theorem	18
2.4.1.10. The Advanced Deficiency Theory	19
3. RESEARCH DESIGN AND METHODS	20

4. RESULTS AND DISCUSSION	22
4.1. Bistability Analysis In Model 1	22
4.1.1. FAS Module	22
4.1.2. Caspase-9 Activation Module.....	26
4.1.2.1. Caspase-9 Activation Module In the Presence of HSP70	26
4.1.2.2. Caspase-9 Activation Module in the Absence of HSP70.....	30
4.2. Bistability Analysis In Model 2	31
4.2.1. Bistability Analysis in ONOO ⁻ Module.....	33
4.2.2. Bistability Analysis in N ₂ O ₃ Module	37
4.2.3. Bistability Analysis in FeL _n NO Module	38
4.3. Model Development	40
4.3.1. Reproduction of Steady States by Using XPPAUT	40
4.3.2. Biological Plausibility of the CRNT Rate Constants	42
4.3.3. Formation of Models.....	47
4.3.4. Analysis Using Bistable Apoptosis Models	49
4.4. Simulations of The Models.....	50
4.4.1. Simulations Using Existing Models.....	50
4.4.2. Analysis on Model 1 (Without NO Effects).....	53
4.4.3. NO Species Formation Model (Model 2).....	54
4.4.4. Analysis on Combined Model (Model 3).....	55
5. CONCLUSIONS AND RECOMMENDATIONS.....	62
5.1. Conclusions.....	62
5.2. Recommendations	64
APPENDIX A: REACTION EXPRESSIONS AND PARAMETERS USED IN THE SIMULATION.....	65
A.1 . Model 1	65
A.2 . Model 2	70
A.3 . Model 3	72
APPENDIX B: DETERMINATION Of CASPASE-3 THRESHOLD VALUE	73
REFERENCES.....	74

LIST OF FIGURES

Figure	2.1.	Forms of cell death adapted from Alberts <i>et al.</i> (2002)	4
Figure	2.2.	Procaspase activation process adapted from Alberts <i>et al.</i> (2002) .	5
Figure	2.3.	Intrinsic and extrinsic apoptotic stimuli adapted from Dash <i>et al.</i> (2003)	6
Figure	2.4.	Major events during DISC formation adapted from Curtin and Cotter (2003)	7
Figure	2.5.	Mitochondria-dependent apoptotic pathway adapted from Bagci <i>et al.</i> (2006)	12
Figure	2.6.	Nitric oxide (NO)-related reactions (Model 2) adapted from Bagci <i>et al.</i> (2008)	13
Figure	2.7.	Nitric oxide (NO)-related reactions integrated into Model I (Model 3)	14
Figure	2.8.	Sample chemical reaction network	16
Figure	2.9.	A weakly reversible network	17
Figure	4.1.	The FAS module adapted from Bagci <i>et al.</i> (2006)	23
Figure	4.2.	Reaction network of FAS-mediated apoptotic pathway	25
Figure	4.3.	Rate constants of the FAS-mediated reaction network	25

Figure 4.4.	Steady state concentrations for the FAS-mediated reaction network	26
Figure 4.5.	The Caspase-9 activation module adapted from Bagci <i>et al.</i> (2006)	27
Figure 4.6.	Reaction network of the caspase-9 activation module	28
Figure 4.7.	Rate constants of the reaction network of the caspase-9 activation module	29
Figure 4.8.	Steady state concentrations for the caspase-9 activation module reaction network	29
Figure 4.9.	Reaction network of the caspase-9 activation module in the absence of HSP70	30
Figure 4.10.	Modules of the NO Pathway adapted from Bagci <i>et al.</i> (2008) (ONOO ⁻ module: Red, N ₂ O ₃ module: Yellow, and FeL _n NO module: Blue)	33
Figure 4.11.	ONOO ⁻ module reaction pathway adapted from Bagci <i>et al.</i> (2008)	34
Figure 4.12.	Normalized reaction rate constants given by CRNT for ONOO ⁻ module	35
Figure 4.13.	Steady states obtained from CRNT analysis for ONOO ⁻ module	35
Figure 4.14.	Eigenvalues of steady state I given for ONOO ⁻ module	36
Figure 4.15.	Eigenvalues of steady state II given for ONOO ⁻ module	36
Figure 4.16.	N ₂ O ₃ module reaction pathway adapted from Bagci <i>et al.</i> (2008)	37

Figure 4.17.	FeL _n NO module reaction pathway adapted from Bagci <i>et al.</i> (2008)	39
Figure 4.18.	Steady state I of caspase-9 activation module	40
Figure 4.19.	Steady state II of caspase-9 activation module	41
Figure 4.20.	Asymptotically stable steady state for ONOO ⁻ module	41
Figure 4.21.	Unstable state for ONOO ⁻ module	41
Figure 4.22.	Apoptotic state of model 1 by Bagci <i>et al.</i> (2008) in the presence of cooperativity in apoptosome formation (p=4)	50
Figure 4.23.	Cell survival state of model 1 by Bagci <i>et al.</i> (2008) in the presence of cooperativity in apoptosome formation (p=4)	51
Figure 4.24.	Apoptotic state of model 3 (including NO effects) by Bagci <i>et al.</i> (2008) in the presence of cooperativity in apoptosome formation (p=4)	51
Figure 4.25.	Apoptotic state of model 3 (including NO effects) by Bagci <i>et al.</i> (2008) in the lack of cooperativity in apoptosome formation (p=1)	52
Figure 4.26.	Apoptotic state of model 1 by Bagci <i>et al.</i> (2008) in the lack of cooperativity in apoptosome formation (p=1)	52
Figure 4.27.	Caspase-3 concentration profile in model 1 ([HSP70] ₀ = 3.15)	53
Figure 4.28.	Caspase-3 concentration profile in model 1 ([HSP70] ₀ = 0.15)	54
Figure 4.29.	Stable steady state solution of model 2	55

Figure 4.30.	Unstable state of model 2	55
Figure 4.31.	Caspase-3 concentration profile in the cell survival state I (simulation of model 311)	56
Figure 4.32.	Caspase-3 concentration profile in the apoptotic state I (simulation of model 312)	58
Figure 4.33.	Caspase-3 concentration profile in the cell survival state II (simulation of model 321)	59
Figure 4.34.	Caspase-3 concentration profile in the apoptotic state II (simulation of model 322)	60

LIST OF TABLES

Table	4.1.	Representation of the species and complexes in the FAS module . .	23
Table	4.2.	Representation of the reactions in the FAS module	24
Table	4.3.	Representation of the species and complexes in the caspase-9 activation module	27
Table	4.4.	Representation of the reactions in the caspase-9 activation module	28
Table	4.5.	The set of reactions containing NO effects on the apoptotic pathway (Bagci <i>et al.</i> , 2008)	32
Table	4.6.	Reactions of ONOO ⁻ module and their letter representations	34
Table	4.7.	Reactions of N ₂ O ₃ module and their letter representations	38
Table	4.8.	Reactions of FeL _n NO module and their letter representations	39
Table	4.9.	Comparison of reaction rate constants given by CRNT and proposed by Bagci <i>et al.</i> (2008) for caspase-9 activation module . .	42
Table	4.10.	Reaction rate constants used for caspase-9 activation module simulation	43
Table	4.11.	Comparison of reaction rate constants given by CRNT and proposed by Bagci <i>et al.</i> (2008) for ONOO ⁻ module	44

Table 4.12.	Comparison of reaction rate constants given by CRNT and proposed by Bagci <i>et al.</i> (2008) for ONOO ⁻ module after unit conversion	46
Table 4.13.	Reaction rate constants used for ONOO ⁻ module simulation	46
Table 4.14.	Mathematical expression of model 1 in terms of ordinary differential equations	48
Table 4.15.	Mathematical expression of model 2 in terms of ordinary differential equations	49
Table 4.16.	Mathematical expressions of additional reactions of model 3 in terms of ordinary differential equations	49
Table 4.17.	Steady state concentrations of critical species in simulation of model 311	57
Table 4.18.	Steady state concentrations of critical species in simulation of model 312	58
Table 4.19.	Steady state concentrations of critical species in simulation of model 321	59
Table 4.20.	Steady state concentrations of critical species in simulation of model 322	60
Table A.1.	Reactions of the mitochondria-dependent apoptosis model (model 1)	65

Table A.2.	Reaction rate constants of the mitochondria-dependent apoptosis model (model 1)	66
Table A.3.	Net formation rate equations of model 1	67
Table A.4.	Formation and degradation rate equations of model 1	67
Table A.5.	Parameters used in simulation of model 1	68
Table A.6.	Initial concentrations of components of model 1	68
Table A.7.	Initial concentrations for obtaining steady state I	69
Table A.8.	Initial concentrations for obtaining steady state II	69
Table A.9.	NO pathway reactions effecting on apoptotic pathway (model 2) . .	70
Table A.10.	Reaction rate constants of model 2	71
Table A.11.	Equilibrium levels and initial concentrations used in model 2	72
Table A.12.	Additional reactions combining model 1 and model 2 (model 3) . .	72
Table A.13.	Rate constants of additional reactions combining model 1 and model 2	72

LIST OF SYMBOLS/ABBREVIATIONS

A	Species of a Network
E	Reaction Vectors
J	Net Formation Rate
k	Reaction Rate Constant
<i>l</i>	Number of Linkage classes
M_{casp3}	Caspase-3 Concentration
N	Number of Caspase-3 Molecules
n	Number of Moles
<i>n</i>	Number of Complexes of a Network
p	Cooperativity
R	Rate of Reaction
R	Radius of the Cell
S	Dimension of Stoichiometric Subspace
V	Volume of the Cell
V^+	Set of Vectors Having No Negative Components
μ	Degradation Rate Constant
δ	Deficiency

θ	Linkage Class
CRNT	Chemical Reaction Network Toolbox
cyt <i>c</i>	Cytochrome <i>C</i>
DISC	Death Inducing Signaling Complex
FADD	FAS-Associated Death Domain
GSH	Glutathione
HSP70	Heat Shock Protein 70
IAP	Inhibitor of Apoptosis Protein
MA	Microaggregate
MPTP	Mitochondrial Permeability Transition Pore Complex
NO	Nitric Oxide
ODE	Ordinary Differential Equations

1. INTRODUCTION

In engineering and science, a mathematical model is a mathematical abstraction of a physical, chemical or biological phenomenon. It is needed to predict the expected behavior of a system using computer simulations which may be an industrial size chemical reactor or a biological process taking place in a cell. Mathematical modeling provides valuable information on the complex dynamics of biological systems, such as testing the expected behavior of a process, helping to design experiments etc. Application of mathematical methods to system behavior enables *in silico* experimenters to investigate a pathway in a wide range of parameters. This is important because it is difficult to determine sensitive kinetic parameters for biological processes. A number of different mathematical representations of the same process can be obtained each differing in sophistication. Scientifically, a model can be said to be adequate if it predicts the experimental findings.

Apoptosis is one of the main types of programmed cell death (PCD) and involves a series of biochemical events leading to a characteristic cell morphology and death. Apoptosis is necessary to shape tissues and organs, it plays an important role for the immune system, and is critical for normal development. It is known that apoptosis is a bistable process since monostable cell survival causes tumor formation, even cancer and monostable cell death causes neurodegenerative illnesses such as Alzheimer's disease and Parkinson's disease. The mathematical term bistability for a dynamical system means that, depending on the initial conditions, the system can move towards two separate states. In the case of a cell, following a series of biochemical reactions and physical interactions, the cell programs itself either to survival or to death. At this point, determination of critical concentrations of important proteins that play vital roles in apoptosis becomes important.

There are a number of mathematical models developed on apoptotic pathways by combining various components that play crucial role in apoptosis. The first mathematical model of caspase activation was proposed by Fussenegger *et al.* (2000), however, their model failed to predict the bistability in the cell. Recent models were reviewed in

Loughran *et al.* (2008). Lavrik *et al.*, (2007) showed that triggering of CD95 (FAS/APO-1) may result both in cell survival or death (bistable response), depending on the strength of the stimulus on their previously developed CD95 mediated apoptosis model. Eissing *et al.*, (2004) suggested that the interplay between caspase-3 activation and inhibitor of apoptosis proteins (IAP) cause bistability in their receptor-induced apoptosis model of Type I cells. Legewie *et al.*, (2006) also found that inhibitors are crucial for the existing of bistability by suppressing the amount of active caspases (caspase-3 and caspase-9) produced. Bentele *et al.*, (2004) proposed a switch model which is not bistable and suggested that a transition from cell survival state to apoptotic state occurs when stimuli for apoptosis are sufficiently high. Stucki and Simon (2005) also predicted that for apoptosis to occur, concentration of caspase-3 should exceed a threshold value. In addition to these, Siechs *et al.* (2002) proposed that Bcl-2 family members and consequent cytochrome c (cyt *c*) release are critical for the induction of apoptosis. Furthermore, Nakabayashi and Sasaki (2006) built a model, which does not involve cooperative binding (increase in the rate of complex binding with the presence of bound complex(es)) in the apoptosome formation. Bistability analysis of a mitochondria-dependent apoptotic pathway was studied by Bagci *et al.* (2006) who used results from nonlinear mechanics to demonstrate the existence of bifurcation in the network. Contrary to Nakabayashi and Sasaki (2006), they suggested that cooperativity in apoptosome formation is required for bistability. In another paper, Bagci *et al.* (2008) have included nitric oxide effects on apoptosis induction into their mathematical model, however, have not investigated bistability. This thesis builds on these two papers, which are reviewed extensively in the “Theoretical Background and Significance” Section. In this study, the work done by Bagci *et al.* (2006) on the bistability of apoptosis and the theory developed for a chemically reacting system to determine multiequilibria are combined to obtain the desired system characteristics such as bistability in a single cell. With this aim, bistability analysis is carried out on the mitochondria-dependent apoptosis model with the addition of nitric oxide effects in the lack of cooperativity in the apoptosome formation.

The thesis comprises five sections. The theoretical information about the apoptosis process, background of the model development and a brief review of chemical reaction network theory are given in the “Theoretical Background and Significance” Section. In “Research Design and Methods” Section, bistability analysis of the modules, model

development and the simulation of the models are explained. Then, the Chemical Reaction Network Toolbox (CRNT) results of bistability analysis in the modules and the outputs of the simulations of the resulting models obtained from XPPAUT are given and discussed in the “Results and Discussion” Section. Finally, the conclusions and recommendations for future studies are given in the “Conclusions and Recommendations” Section. Some system parameters are presented in the appendices.

2. THEORETICAL BACKGROUND AND SIGNIFICANCE

2.1. Apoptosis

Apoptosis, also known as *Programmed Cell Death*, in which a "suicide" program is activated within the cell, is a normal phenomenon, occurring frequently in a multicellular organism. In contrast to apoptosis, uncontrolled cell death leads to lysis of cells, inflammatory responses and, potentially, to serious health problems in another form of (pathological) cell death called *necrosis*. In necrosis, cells spill their contents to extracellular medium. However, a cell that undergoes apoptosis dies neatly, without damaging its neighbors as it can be seen from Figure 2.1. The cell shrinks and condenses. The cytoskeleton collapses, the nuclear envelope disassembles, and the nuclear DNA breaks up into fragments (Alberts *et al.*, 2002).

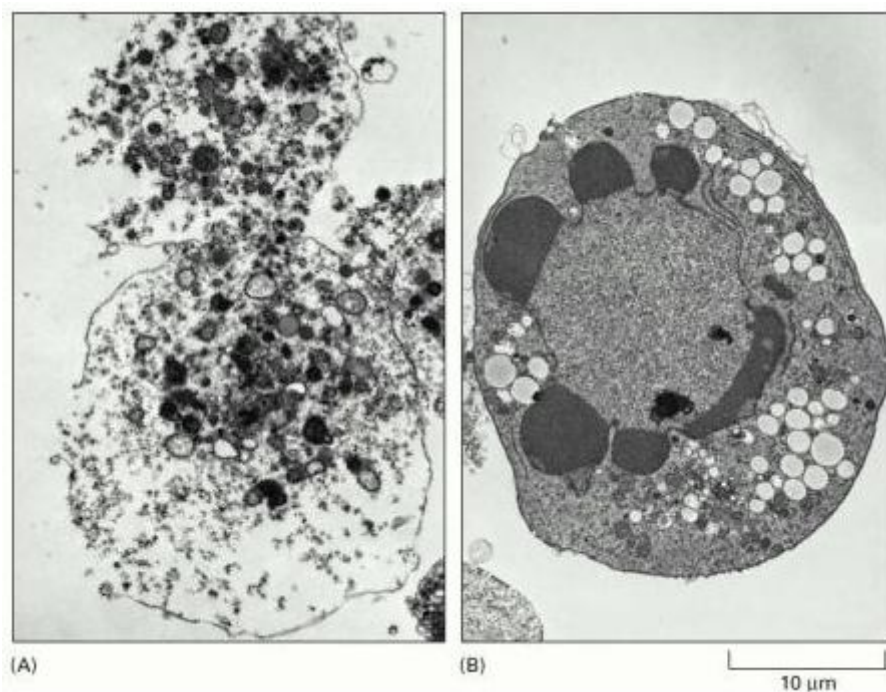


Figure 2.1. Forms of cell death adapted from Alberts *et al.* (2002)

(A) Necrosis (B) Apoptosis in a culture dish. Cell in (A) seems to be exploded, whereas cell in (B) has condensed but seems relatively intact.

The intracellular machinery responsible for apoptosis seems to be similar in all animal cells. This machinery depends on a family of aspartate-directed cysteine enzyme proteases known as caspases, which are typically activated in the early stages of apoptosis. Caspases are synthesized as inactive precursors called procaspases or zymogens. DNA damage and death receptor activation cause cleavage and activation of procaspases as shown in Figure 2.2. The activation of the caspases enables onset of necessary processes for apoptosis and enables phagocytic removal of the cell (Eissing *et al.*, 2004). These proteins breakdown or cleave key cellular components that are required for normal cellular function including structural proteins in the cytoskeleton and nuclear proteins such as DNA repair enzymes. The caspases can also activate other degradative enzymes such as DNases, which begin to cleave the DNA in the nucleus. There are two types of apoptotic caspases: Initiator caspases (e.g. caspase-2, caspase-8, caspase-9 and caspase-10) and executioner caspases (e.g. caspase-3, caspase-6, caspase-7).

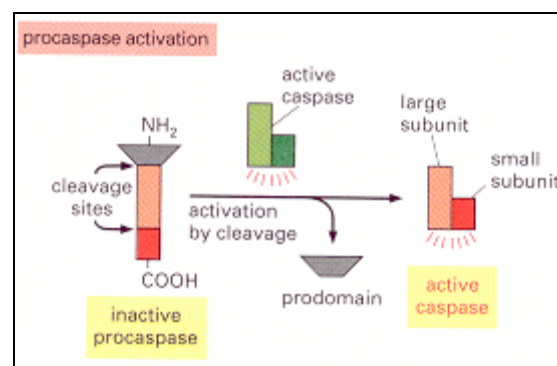


Figure 2.2. Procaspase activation process adapted from Alberts *et al.* (2002)

There are a number of apoptosis induction mechanisms, through which apoptosis can be induced in cells. In some cases, apoptosis can be initiated following intrinsic signals that are produced following cellular stress. Cellular stress may occur from exposure to radiation or chemicals or to viral infection. It might also be a consequence of growth factor deprivation or oxidative stress caused by free radicals as shown in Figure 2.3.

The sensitivity of cells to any of these stimuli can vary depending on a number of factors such as the expression of pro- and anti-apoptotic proteins (e.g. the Bcl-2 proteins or the Inhibitor of Apoptosis Proteins (IAP)), the severity of the stimulus and the stage of the cell cycle (Alberts *et al.*, 2002). In general, intrinsic signals initiate apoptosis via the

involvement of the mitochondria. The relative ratios of the various Bcl-2 proteins can often determine how much cellular stress is necessary to induce apoptosis (Packham and Stevenson, 2005).

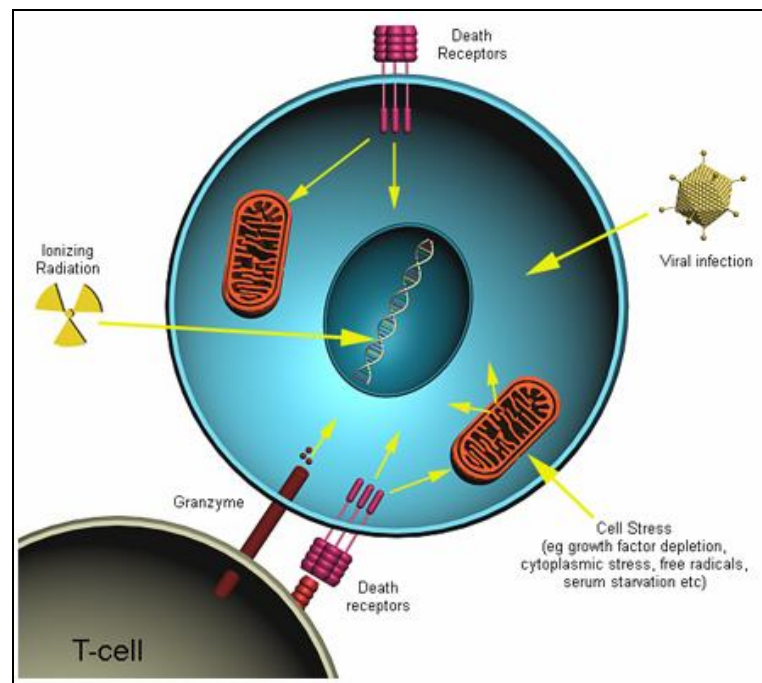


Figure 2.3. Intrinsic and extrinsic apoptotic stimuli adapted from Dash *et al.* (2003)

In other cases, procaspase activation can be triggered from outside the cell by the activation of death receptors on the cell surface. Death receptors belong to a superfamily of receptors called the Tumor Necrosis Factor (TNF) superfamily. They are involved in proliferation, differentiation and apoptosis. Each receptor can bind with one or more than one type of ligand. Receptor trimerization is induced by binding of ligand to receptor and clustering on the plasma membrane. Trimerization is required to initiate apoptosis (Curtin and Cotter, 2003). The large scale clustering helps to amplify the apoptotic signaling. Some cells can still trigger apoptosis in the absence of receptor clustering, such as lymphocytes, but amplification of the signaling pathway is necessary for full apoptotic response in most cases. In addition to death receptors, there are also decoy receptors which possess functional extracellular ligand binding domains but no intracellular death domains that are required to recruit adaptor proteins needed for apoptosis, so that they inhibit binding of a ligand to its normal receptor.

2.2. FAS Mediated Apoptosis

Activation of FAS receptor by FAS ligand initiates a caspase cascade needed for apoptosis. Effective formation of a protease complex called DISC (Death Inducing Signaling Complex) is required in FAS-mediated apoptosis. Following FAS receptor ligation with FAS ligand, microaggregates of FAS receptor form on the cell surface independent of caspase activity. Trimerization of FAS receptor is the minimal event required for FADD (FAS-Associated Death Domain) recruitment and effective DISC formation. Activation of caspase-8 occurs following DISC formation and directly regulates the formation of large FAS receptor aggregates on the plasma membrane of cells and increased DISC activity (Özören and El-Deiry, 2002). Assembly of the components of the FAS, DISC is a highly organized event and involves sequential clustering of adaptor and executioner proteins at FAS receptor aggregates as shown in Figure 2.4. FADD binds to the intracellular death domain of FAS receptor in response to receptor trimerization (Curtin and Cotter, 2003). Caspase-8 and bound FADD are recruited to the plasma membrane and the increased local concentration of these proteases induces autocleavage and activation of caspase-8. Caspase-8 appears to be the principal initiator.

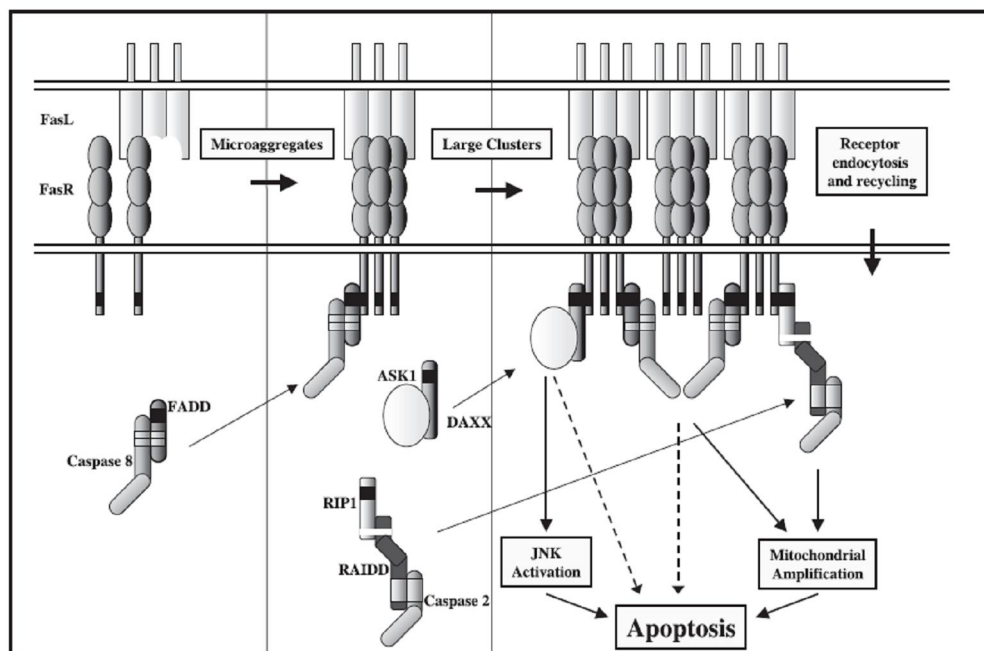


Figure 2.4. Major events during DISC formation adapted from Curtin and Cotter (2003)

Active caspase-8 can directly cleave and activate executioner caspases in type I cells. However, amplification of apoptosis is required since very little caspase-8 is activated in type II cells. In type II cells, the activation cascade is amplified via the mitochondria (Bagci *et al.*, 2006). Cleavage of the Bcl-2 family member BID by caspase-8 produces the pro-apoptotic tBID fragment that induces cytochrome *c* release from mitochondria and caspase-9 activation (Özören and El-Deiry, 2002). Expression of anti-apoptotic Bcl-2 family members can regulate the sensitivity of mitochondria to tBID and in turn the sensitivity of type II cells to FAS-mediated apoptosis.

Since, dysfunction of the regulatory mechanisms in FAS receptor signaling can cause autoimmune disease and cancer, FAS receptor signaling is crucial for the healthy functioning of the cells. A soluble decoy receptor called DcR3 was identified to bind with FAS ligand. The gene coding for DcR3 is located on chromosome 20, which is often amplified in colon cancer. DcR3 inactivates membrane-bound FAS ligand on adjacent cells, prevents activation of FAS receptor and hence promotes tumor survival (Curtin and Cotter, 2003). Expression of FADD can also regulate the sensitivity of cells to FAS-mediated apoptosis by altering the levels of executioner caspases cleaved in response to FAS receptor activation. Even though FADD is a key component of FAS receptor signaling, expression is rarely decreased in tumor cells because expression of FADD is also required for cell cycle progression. In contrast to FADD, the expression of caspase-8 is often decreased in cells resistant to FAS-mediated apoptosis (Curtin and Cotter, 2003).

A common mechanism employed by cells to increase or decrease the sensitivity to FAS-mediated apoptosis is the regulated cell surface expression of FAS receptor and FAS ligand. Alternative splicing, protease-mediated cleavage, gene expression and sequestering of FAS receptor and FAS ligand have been found to regulate FAS-mediated apoptosis.

FAS receptor is expressed at a single locus on chromosome 10 in human cells and chromosome 19 in mouse cells (Curtin and Cotter, 2003). At least eight splice variants and seven distinct isoforms of FAS receptor have been identified in human cells and arise from alternative splicing of FAS receptor RNA. Only isoform 1 encodes the functional, full-

length protein and it is 335 amino acids in length. It consists of three cysteine-rich pseudo-repeats, a transmembrane domain and an intracellular death domain. Isoform 2 is 314 amino acids in length and encodes three cysteine-rich regions and a death domain, but is missing a transmembrane region. Isoforms 4 through 7 are also missing a transmembrane region and these soluble isoforms of FAS receptor may sequester and inactivate FAS ligand on adjacent cells and infiltrating cytotoxic T lymphocytes (Curtin and Cotter, 2003).

Overexpression of soluble FAS receptor has been implicated with the progression of prostate cancer. Isoform 3 is 220 amino acids long and contains three cysteine-rich pseudorepeats and a transmembrane region, but the cytoplasmic domain is truncated and does not contain a functional death domain. Overexpression of this isoform occurs in foetal thymocytes and may account for the high resistance in these cells to apoptosis following FAS receptor aggregation (Curtin and Cotter, 2003).

2.3. Apoptosis Models

2.3.1. Bistability and Apoptosis

Several signal transduction pathways governing cell fate decisions have experimentally and theoretically been shown to display a bistable behavior (Xiong and Ferrell, 2003). Bistability is also an obvious and mandatory property of the apoptotic machinery, as the status “alive” must be stable (Tyson *et al.*, 2003). In a healthy human cell, bistability condition must prevail as this means either cell survival or apoptosis. Also, caspases are known to possess zymogenicity (the ratio of the activities of the processed caspase to its inactive precursor) (Stennicke and Salvesen, 1999) and partial activation is observed in some physiological processes (Newton and Strasser, 2003). However, if the apoptotic initiation signal is beyond a certain threshold, the cell must irreversibly enter the pathway to develop apoptosis. Therefore, bistability is taken as an “essential condition” to evaluate possible models with respect to this expected behavior.

2.3.2. A Mitochondria-Dependent Apoptosis Model

Mitochondria play an important role in the regulation of cell death. Following the formation of pores in the mitochondrial membrane called the Mitochondrial Permeability Transition Pores (MPTPs), cytochrome *c* is released from mitochondria. These pores are thought to form through the action of the pro-apoptotic members of the Bcl-2 family of proteins, which in turn are activated by apoptotic signals such as cell stress, free radical damage or growth factor deprivation. Mitochondria also play an important role in amplifying the apoptotic signaling from the death receptors, with receptor recruited caspase-8 activating the pro-apoptotic Bcl-2 protein, Bid (Özören and El-Deiry, 2002).

The Bcl-2 family of proteins is involved in the regulation of apoptosis. Some of these proteins (such as Bcl-2 and Bcl-XL) are anti-apoptotic, while others (such as Bad, Bax or Bid) are pro-apoptotic. The sensitivity of cells to apoptotic stimuli can depend on the balance of pro- and anti-apoptotic Bcl-2 proteins. When there is an excess of pro-apoptotic proteins the cells are more sensitive to apoptosis, in contrast when there is an excess of anti-apoptotic proteins the cells will tend to be more resistant. An excess of pro-apoptotic Bcl-2 proteins at the surface of the mitochondria is thought to be important in the formation of the MPTP (Siehs *et al.*, 2002).

The pro-apoptotic Bcl-2 proteins are often found in the cytosol where they act as sensors of cellular damage or stress. Following cellular stress they relocate to the surface of the mitochondria where the anti-apoptotic proteins are located. This interaction between pro- and anti-apoptotic proteins disrupts the normal function of the anti-apoptotic Bcl-2 proteins and can lead to the formation of pores in the mitochondria and the release of cytochrome *c* and other pro-apoptotic molecules from the intermembrane space. This in turn leads to the formation of the apoptosome and the activation of the caspase cascade.

The release of cytochrome *c* from the mitochondria is a particularly important event in the induction of apoptosis. Once cytochrome *c* has been released into the cytosol it is able to interact with a protein called Apaf-1. This leads to the recruitment of procaspase-9

into a multi-protein complex with cytochrome *c* and Apaf-1 called the apoptosome. Formation of the apoptosome leads to activation of caspase-9 and the induction of apoptosis by activating executioner caspases; caspase-3, caspase-6 and caspase-7 (Ryu *et al.*, 2009).

Bagci *et al.* (2006) developed the bistable mitochondria-dependent apoptosis model shown in Figure 2.5 in terms of coupled ordinary differential equations resulting from mass action kinetics. The model contains reaction equations starting from caspase-8 activation due to DISC formation. Caspase-8 provides the cleavage of Bid. Active tBid and Bax on the mitochondria membrane provides to release of cytochrome *c* (cyt *c*) from mitochondria. Cooperative binding of Apaf-1/cyt *c* complexes results with the formation of apoptosome, then procaspase-9 recruits to apoptosome and becomes activated. The activation of caspase-9 and hence executioner caspase-3 is critical for the onset of apoptosis. In Figure 2.5., there are some inhibitors in the pathway. For example, IAP inhibits caspase-3, caspase-9 and the holoenzyme. Bcl-2 represents the anti-apoptotic effects of Bcl-2 family members. p53 upregulates apoptosis by promoting Bax and suppressing Bcl-2. Caspase-3 activates Bid via a feedback mechanism and also promotes Bax indirectly by suppressing Bcl-2.

In this model, kinetic cooperativity in apoptosome assembly is the key element to achieve bistability. This cooperativity in apoptosome formation is critical for determining the healthy responses to apoptotic stimuli. Moreover, simulation results show that Bax degradation rate is important for the pathological state of the cell. For instance, if Bax degradation rate is above a threshold value or Bax expression rate is below a threshold value, then cells will exhibit monostable cell survival (i.e. no apoptosis). On the other hand, caspase-3 (executioner caspase) concentration of the cell will determine whether cell death occurs or not.

Additionally, it is also shown that if the number of mitochondrial permeability transition pores (MPTPs) exceeds a threshold value, this situation may cause monostable apoptotic response. Finally, by reducing the number of model equations to low dimensions,

the robustness of possible mechanisms of bistability is analyzed by using tools of nonlinear dynamics (Bagci *et al.*, 2006).

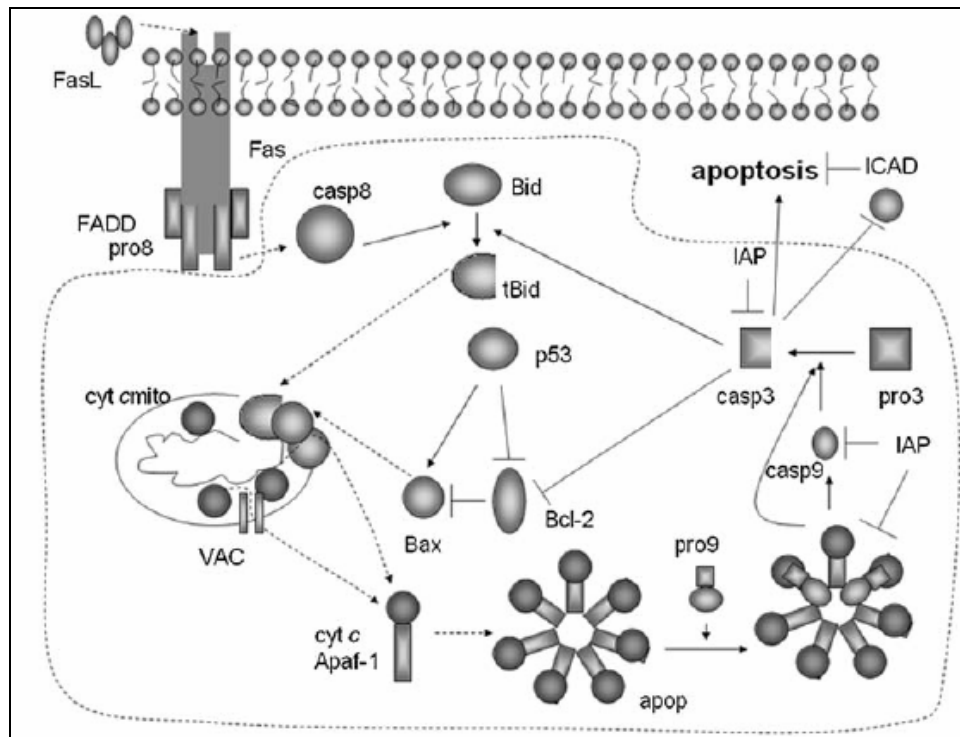


Figure 2.5. Mitochondria-dependent apoptotic pathway adapted from Bagci *et al.* (2006)

2.3.3. Nitric Oxide Effects on the Mitochondria-Dependent Apoptosis Model

In another paper, Bagci *et al.* (2008) also showed the role of nitric oxide (NO) on the mitochondria-dependent apoptotic pathway. In their mathematical model, NO-related reactions (Figure 2.6) are integrated into the mitochondria-dependent apoptosis model and are given Figure 2.7 (Bagci *et al.*, 2008). The kinetic parameters of the simulations were selected from a wide parameter range in the literature (Hu *et al.*, 2006). Computations on this model aim to understand the regulatory effect of the reactive NO species namely N_2O_3 , non-heme iron nitrosyl species (FeL_nNO), and peroxynitrite ($ONOO^-$). According to their simulation results, these NO species, and their interplay with glutathione (GSH), have either net anti-apoptotic or pro-apoptotic effects at long time scales.

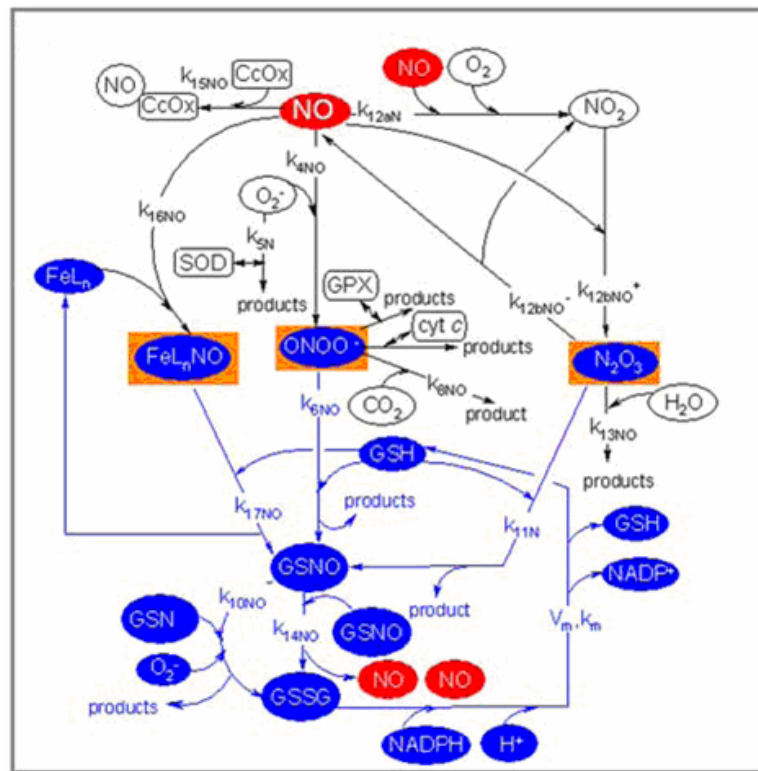


Figure 2.6. Nitric oxide (NO)-related reactions (Model 2) adapted from Bagci *et al.* (2008)

In Figure 2.6, it is shown that NO species N_2O_3 , FeL_nNO and $ONOO^-$ are produced from the reactions of highly reactive NO with O_2 , non-heme iron (FeL_n) and superoxide (O_2^-) respectively. GSH modulates concentrations of NO species by reacting with them. GSH is converted by these reactions to nitrosogluthathione (GSNO), which is then converted to glutathione disulfide (GSSG) and finally back to GSH. There is also NO recycle in the pathway. NO is converted to NO species and then produced back during reduction of GSH to GSSG.

Simulations suggest that when the non-heme iron concentration is higher than a threshold value, caspase-3 levels always decrease to zero, and the rate of this decay depends on the initial concentrations of caspase-8 and glutathione. Note that zero caspase-3 concentration level results in cell survival. However, if the initial concentration of glutathione is sufficiently high, then executioner caspase concentrations can reach apoptotic levels independent of the non-heme iron concentration. It was also observed that although N_2O_3 does not eliminate the bistability between cell survival and cell death, it increases the initial threshold value of caspase-8 for the onset of apoptosis. On the other

hand, experimental studies show that ONOO^- may induce opening of mitochondria permeability transition pores and subsequent *cyt c* release from mitochondria (Kim *et al.*, 2001) as shown in Figure 2.7. This experimental result is consistent with the simulations and proves that ONOO^- has a pro-apoptotic effect. Moreover, anti-apoptotic effects of N_2O_3 and FeL_nNO are shown in Figure 2.7. It is known that N_2O_3 inhibits caspase-8 activation and FeL_nNO inhibits caspase-3 and caspase-9 (Kim *et al.*, 2001).

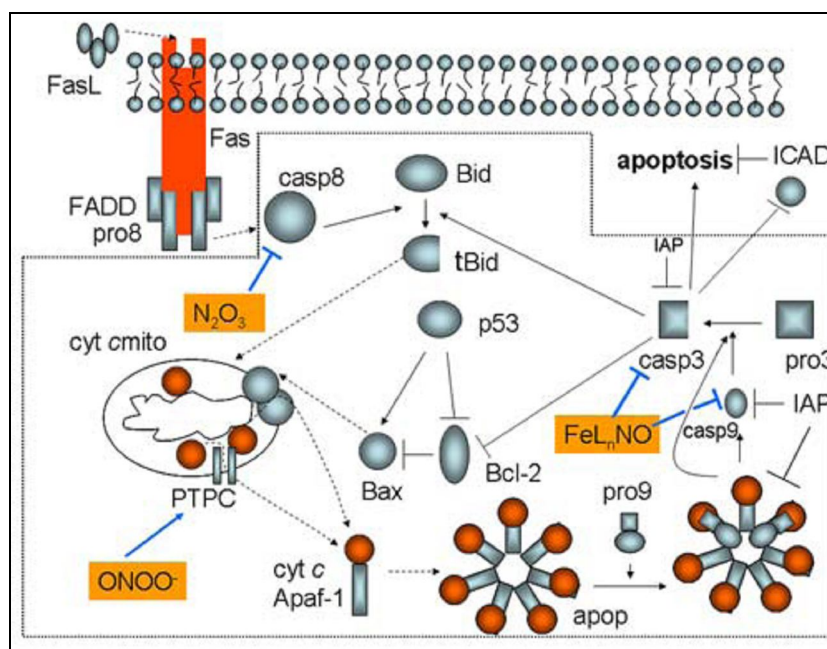


Figure 2.7. Nitric oxide (NO)-related reactions integrated into Model I (Model 3)
adapted from Bagci *et al.* (2008)

Bagci *et al.* (2008), obtained bistability in the mitochondria-dependent apoptosis model in the presence of cooperativity (reaction order of heptamer formation from monomers) in the apoptosome formation. Their simulation results suggest that the model is monostable in the case of lack of cooperativity, $p=1$, in the apoptosome formation. However, there is controversy over the numerical value of the cooperativity parameter, p , in the literature. While some authors assume $p=1$ (no cooperativity), others assume $p>1$ (Ryu *et al.*, 2009). Lack of cooperativity is plausible biologically in the apoptosome formation, since apoptosome is formed by successive addition of Apaf-1/*cyt c* complex and presence of one complex does not increase the rate of binding of others (Nakabayashi and Sasaki, 2006). Hence, in this study, reaction rate constants that will represent the bistable character of the apoptotic pathway are determined by using Chemical Reaction

Network Theory, (Feinberg, 1977) new reactions are added to the previous model studied by Bagci *et al.* (2008), this updated model is simulated by using a package program XPPAUT developed to interpret a system of nonlinear Ordinary Differential Equations (ODEs) by Ermentrout and components of the resulting model are analyzed for different ideal cell types.

2.4. Chemical Reaction Network Theory

Biological networks have great complexity because of the large number of interacting components. The dynamics and functioning of these systems can be understood not only by biological intuition, but also with the help of mathematical modeling. Network topology and reaction mechanisms may cause uncertainty in the process of building a mathematical model due to the existence of several candidate networks. Mathematical modeling basically consists of the development of families of differently structured models followed by a model discrimination step. Experimental knowledge about the existence of multistationarity is a critical evidence for the process of model discrimination of an apoptosis model. Chemical Reaction Network Toolbox (CRNT) developed by Feinberg (1995), connects qualitative properties of ordinary differential equations corresponding to a reaction network to the network structure. It gives information on whether or not multistationarity is possible and, if possible, provides a pair of steady states and the corresponding parameter vector i.e. reaction rate constants. In particular, its assertions are independent of specific parameter values and its only assumption is that all kinetics is of mass-action form. The theory introduces new concepts, such as the *deficiency*, *linkage classes* etc. of a reaction network, and gives conditions on such networks for the existence, uniqueness, multiplicity and stability of fixed points. What follows is adapted from Feinberg (1977).

2.4.1. Reaction Networks and Their Structure

2.4.1.1. Complexes of a Network. The complexes of a network are the entities that appear after and before the reaction arrows. For example in the following chemical reaction network,

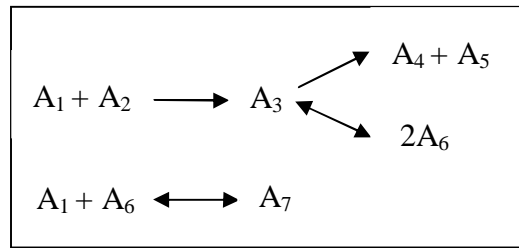


Figure 2.8. Sample chemical reaction network

The complexes are $\{A_1 + A_2, A_3, A_4 + A_5, 2A_6, A_1 + A_6, A_7\}$, and the number of complexes of this network, n , is six.

2.4.1.2. The Reaction Vectors for a Network. Associated with each reaction of an N species network there is a reaction vector in N dimensional Euclidean space \mathbb{R}^N formed by subtracting the "reactant" complex vector from the "product" complex vector. For example, the full set of six reaction vectors for the network above is

$$\{e_3 - e_1 - e_2, e_4 + e_5 - e_3, 2e_6 - e_3, e_3 - 2e_6, e_7 - e_1 - e_6, e_1 + e_6 - e_7\} \quad (2.1)$$

where e_i is an element of \mathbb{R}^N and has one in the i^{th} place and zero in all other places.

2.4.1.3. The Stoichiometric Subspace for a Network. The stoichiometric subspace of an N species network is the linear subspace comprised of all possible linear combinations of the reaction vectors set. The dimensions of the stoichiometric subspace are denoted by s , which is the number of elements in the largest linearly independent set composed of reaction vectors for the network. For the network above,

The reaction vectors $\{e_3 - e_1 - e_2, e_4 + e_5 - e_3, 2e_6 - e_3, e_1 + e_6 - e_7\}$ cannot be obtained as the combinations of each others, so they are linearly independent.

Hence, $s = 4$. i.e. among six vectors (reactions), four vectors (reactions) are linearly independent.

2.4.1.4. The Linkage Classes of a Network. Number of linkage classes of a network is the number of disconnected pieces of its standard reaction diagram.

The number of linkage classes, l , in Figure 2.8 is two, since there are two disconnected pieces in standard reaction diagram.

2.4.1.5. Mass Action Kinetics. Mass action kinetics states that the rate of an elementary reaction (a reaction that proceeds through only one transition state that is one mechanistic step) is proportional to the product of the concentrations of the participating molecules. Assuming mass action kinetics form to investigate the multistationarity (for at least one set of parameter values) for a given biological network is useful when the structure of the network, but not the kinetic parameters, is known.

2.4.1.6. Weakly Reversible Networks. The network is weakly reversible, whenever there is a directed arrow pathway (consisting of one or more arrows) "pointing" from one complex to another, and there is a directed arrow pathway "point" from the second complex to the first. (Equivalently, a network is weakly reversible if in the standard reaction diagram each reaction arrow is contained in a directed reaction cycle.)

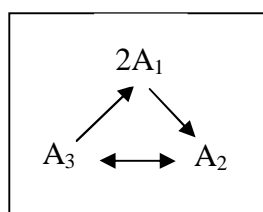


Figure 2.9. A weakly reversible network

In the network above, since there is a directed arrow path connecting $2A_1$ back to A_3 (via A_2), then this network is weakly reversible.

2.4.1.7. The Deficiency of a Network. The number δ , deficiency, is defined by $\delta = n - l - s$, where n represents the number of complexes of a network, l the number of its linkage classes, and s the dimension of its stoichiometric subspace.

2.4.1.8. The Deficiency Zero Theorem. Deficiency Zero Theorem is due to Feinberg, (1987). Consider a mechanism for which the number of complexes is n , the number of linkage classes is l , and the stoichiometric subspace has dimension s . Suppose that $n - l - s = 0$; that is, suppose that the mechanism has deficiency zero ($\delta=0$). Then the following statements are true:

- If the mechanism is not weakly reversible, then for arbitrary kinetics (mass action or otherwise), the induced dynamic equations cannot give rise to an equilibrium in V^+ where V^+ is the set of all vectors of \mathbb{R}^N which have no negative components.
- If the mechanism is not weakly reversible, then for arbitrary kinetics (mass action or otherwise), the induced dynamic equations cannot give rise to a composition cycle in V^+ containing a point in V^+ .
- If the mechanism is weakly reversible, then for the mass action kinetics with any choice of positive rate constants there exists in each stoichiometric compatibility class of V^+ exactly one equilibrium composition, every equilibrium composition in V^+ is asymptotically stable. Relative to the stoichiometric compatibility class in which it resides, and the dynamic equations cannot give rise to a composition cycle in V^+ . In short, weakly reversible mechanism with zero deficiency gives rise to monostability i.e. one equilibrium point.

2.4.1.9. The Deficiency One Theorem. Consider a weakly reversible network with l linkage classes. Let δ denotes the deficiency of the network; let δ_θ denotes the deficiency of the $\delta_\theta^{\text{th}}$ linkage class, $\theta=1,2,\dots,l$; and suppose that both of the following conditions are satisfied:

$$\delta_\theta \leq 1, \theta = 1, 2, \dots, l \quad (2.2)$$

$$\delta = \sum_{\theta=1}^l \delta_\theta. \quad (2.3)$$

If the network is endowed mass action kinetics, then, for every set of rate constants, the induced differential equations admit precisely one equilibrium in each positive

stoichiometric compatibility class. For a weakly reversible network, if there is only one linkage class, then the induced differential equations can admit multiple equilibria within a positive stoichiometric class only if, the deficiency of the network is two or more.

2.4.1.10. The Advanced Deficiency Theory. The term advanced deficiency is used when deficiency of a network is greater than one. The advanced deficiency theory has the capability to analyze any network that falls outside the scope of deficiency one theory (Ellison and Feinberg, 2000). As with deficiency one theory, the advanced deficiency theory will determine if a network does not have the qualitative capacity to support multiple steady states. Addition of the advanced deficiency theory one can now use reaction network theory to analyze a greater range of mechanisms, including multiple-pathway mechanisms.

3. RESEARCH DESIGN AND METHODS

The objective of this study is to determine whether the mitochondria-dependent apoptosis model with Nitric Oxide (NO) effects has bistable character when there is no cooperativity, since bistability of a cell is essential for a healthy person. This analysis will be carried out using a Chemical Reaction Network Toolbox (CRNT). This DOS program uses certain results in chemical reaction network theory developed by Feinberg (1977). Chemical Reaction Network Theory deals with the relationship between reaction network structure and qualitative properties of the corresponding differential equations. For example, in response to a user-specified reaction network, CRNT tries to determine if there can be positive rate constants and positive initial concentrations of the reacting species such that the resulting differential equations admit multiple steady states. However, the numbers of species and complexes that can be entered to CRNT are limited to 20. For a complex biological process such as apoptosis pathway, the number of complexes involved is much higher than 20. Therefore, it is necessary to decompose the model into modules (compartments). To create a module, first, the reactions are arranged in their biological/chemical order of occurrence so that their formed sequence is causally related. A module is built in such a way that the input species of a module is the output species of the previous one. A sequence of reactions is chosen as a module if a reacting complex or species later appears as a product. This phenomenon is termed as circularity and will probably induce the feedback which is essential for multiplicity (Saez-Rodriguez, 2008). For example, in NO modules (which are referred to as Model 2 in the sequel) different pathways can be chosen (all including the glutathione (GSH) cycle) starting from NO and later producing NO after GSH cycle (antioxidant effect) to complete the circularity condition.

Additionally, circularity is not a required condition to induce multiplicity in a module. It is possible that if a product is inhibited, this may also cause multiplicity and is found in a module chosen starting from apoptosome (which is inhibited by HSP70) to caspase-9 activation. This module is referred to as “caspase-9 activation module” in Figure 4.5. Decomposition renders the bistability analysis using CRNT possible without

decreasing the dimensionality of the pathway (Bagci *et al.*, 2006) and yields more accurate results about the critical concentrations of the species.

The bistability in the mitochondria-dependent apoptosis model is investigated in three models. Model 1 which does not include NO effects; model 2 only includes NO effects namely N_2O_3 , peroxynitrite ($ONOO^-$) and non-heme iron-nitrosyl species (FeL_nNO) and model 3 which gives the big picture by combining model 1 and model 2.

When analyzing the three models, first, different modules preserving causality and circularity or product inhibitions in the models are found and then checked for bistability. If the network in the model does have capacity for multiple steady state as the result of the CRNT analysis, the reaction rate constants of the reactions in the network are taken directly from CRNT program. It should be noted that multiplicity is found only in a small subset of the overall reaction pathway using CRNT, which only quantitatively determines whether a given set of reactions has the capability to yield multiplicity while providing plausible rate constants. Therefore, the dynamical equations arising from mass action kinetics for the reactions used in the module are input into an ordinary differential equation (ODE) solver, XPPAUT developed by Ermentrout (2002). The validation is made if an affirmative result is obtained from XPPAUT. Following this, the remaining differential equations are added one by one and bistability is checked each time a new reaction is added to finally obtain the overall equations in the apoptotic pathway. The reaction rate constants of these reactions are taken from the literature (Bagci *et al.*, 2008) and (Hu *et al.*, 2006). This procedure is performed for both model 1 and 2 and they are later combined to form model 3 which contains set of reactions for the mitochondria-dependent apoptosis model containing NO effects in the absence of cooperativity.

4. RESULTS AND DISCUSSION

4.1. Bistability Analysis In Model 1

The whole apoptosis model (model 3) is composed of two models:

- Model 1: Mitochondria-dependent apoptosis model
- Model 2: Nitric oxide effects on the apoptosis model

First, the bistability in the mitochondria-dependent apoptosis model (model 1) is investigated. Bistability analysis is carried out for different modules chosen to have causality and circularity. Especially, the presence of positive feedback (PF) is a known requirement for multistability (Saez-Rodriguez *et al.*, 2008). Most of the modules do not have capacity for multiple steady states, so they are not critical for the existence of the bistable character of the apoptotic pathway. According to CRNT analysis, only FAS module and caspase-9 activation module do have capacity for multiple steady states.

4.1.1. FAS Module

The equations of FAS module are derived from the ligand induced apoptotic pathway proposed by Curtin and Cotter (2003). The bistability analysis is then carried out on this reaction set. The reactions and components taking place in FAS-mediated apoptosis are given in Figure 4.1 and are taken from Bagci *et al.* (2006). In order to enter the reactions into CRNT, each component is represented by a letter (Table 4.1).

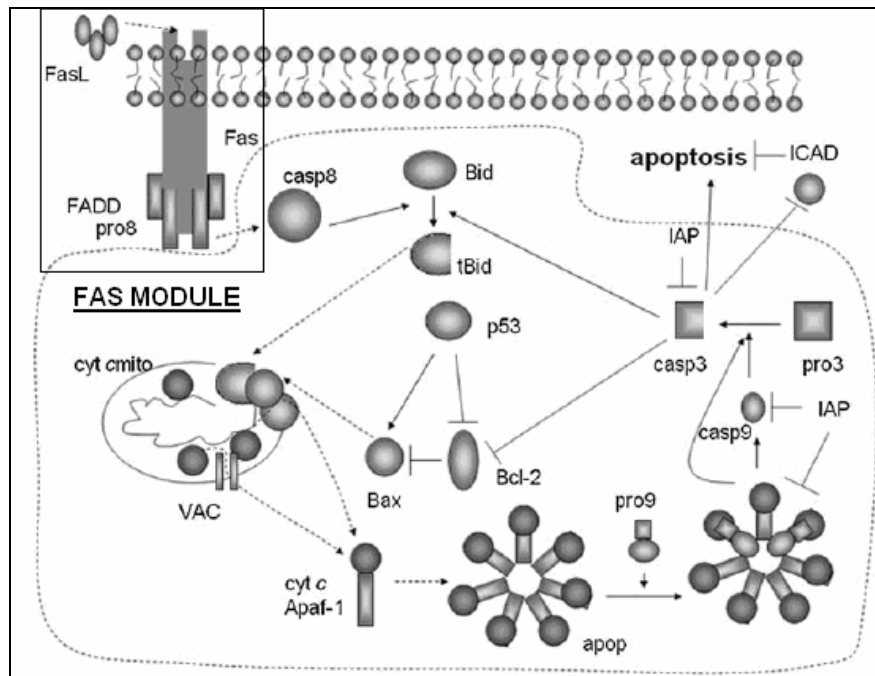


Figure 4.1. The FAS module adapted from Bagci *et al.* (2006)

In this table, FasR represents the functioning FAS receptor having a transmembrane domain and an intracellular death domain. Other isoforms of the FAS receptor with missing transmembrane are denoted by FasR2. FAS ligand-FAS receptor complexes, $(FasL)_3(FasR)_2FasR2$ (D) and $(FasL)_3FasR(FasR2)_2$ (E) are inactive complexes, that cannot transmit the extrinsic signal into the cell. On the other hand, the formation of $(FasL)_3(FasR)_3$ (I) is necessary for the formation of DISC complex, hence the activation of caspase-8.

Table 4.1. Representation of the species and complexes in the FAS module

FasL \rightarrow A	$(FasL)_3(FasR)_3 \rightarrow$ I
$(FasL)_3 \rightarrow$ B	FADD \rightarrow J
FasR \rightarrow R	Pro8 \rightarrow K
FasR2 \rightarrow C	FADD·Pro8 \rightarrow L
$(FasL)_3(FasR)_2FasR2 \rightarrow$ D	MA \rightarrow M
$(FasL)_3FasR(FasR2)_2 \rightarrow$ E	DISC \rightarrow N

In addition to the reaction pathway in the FAS module, the formation and degradation rates of the components are also entered into the program. If a species is used in the reaction pathway without being produced in the pathway, then the formation reaction of that species is added. Degradation of a species is added, if that species is produced in the pathway, but not used as a reactant of any other reaction in the pathway. The set of reactions in the FAS Module and the corresponding symbols used to represent them are given in Table 4.2. For example $0 \Rightarrow A$ means the formation of A and $D \Rightarrow 0$ means the degradation of D.

Table 4.2. Representation of the reactions in the FAS module

$0 \Rightarrow FasL$	$0 \Rightarrow A$
$0 \Rightarrow FasR$	$0 \Rightarrow R$
$0 \Rightarrow FasR2$	$0 \Rightarrow C$
$0 \Rightarrow FADD$	$0 \Rightarrow J$
$0 \Rightarrow Pr o8$	$0 \Rightarrow K$
$3FasL \Leftrightarrow (FasL)_3$	$3A \Leftrightarrow B$
$(FasL)_3 + 2FasR + FasR2 \Leftrightarrow (FasL)_3(FasR)_2FasR2$	$B + 2R + C \Leftrightarrow D$
$(FasL)_3 + FasR + 2FasR2 \Leftrightarrow (FasL)_3FasR(FasR2)_2$	$B + R + 2C \Leftrightarrow E$
$(FasL)_3 + 3FasR \Leftrightarrow (FasL)_3(FasR)_3$	$B + 3R \Leftrightarrow I$
$FADD + Pr o8 \Leftrightarrow FADD \cdot Pr o8$	$J + K \Leftrightarrow L$
$FADD \cdot Pr o8 + (FasL)_3(FasR)_3 \Leftrightarrow MA$	$L + I \Leftrightarrow M$
$2MA \Leftrightarrow DISC$	$2M \Leftrightarrow N$
$(FasL)_3(FasR)_2FasR2 \Rightarrow 0$	$D \Rightarrow 0$
$(FasL)_3FasR(FasR2)_2 \Rightarrow 0$	$E \Rightarrow 0$
$DISC \Rightarrow 0$	$N \Rightarrow 0$

The reactions of the FAS module are entered into the CRNT program as shown in Figure 4.2. The reactions given in the second column of Table 4.2 are rearranged by CRNT such that first the formation reactions, followed by degradation reactions and then biochemical reactions and physical interactions are written in the order of their occurrence.

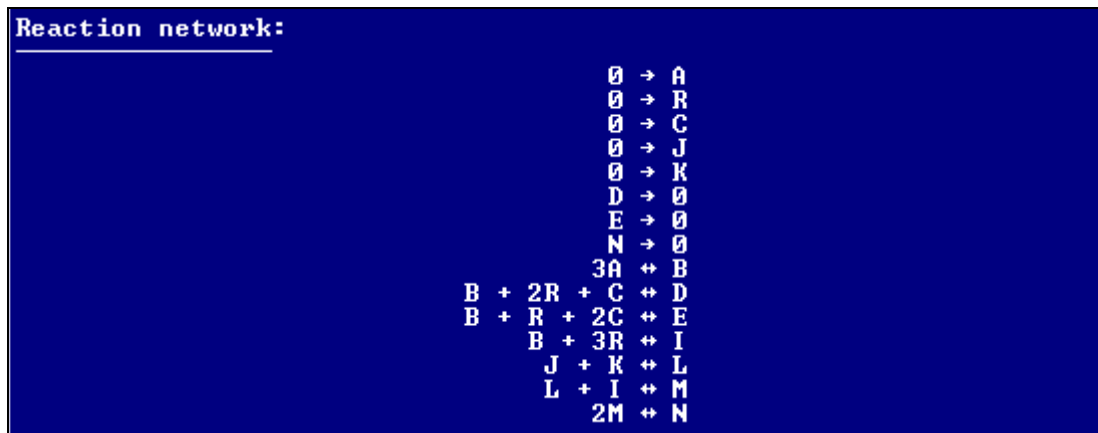


Figure 4.2. Reaction network of FAS-mediated apoptotic pathway

This reaction network given in Figure 4.2 does have capacity for multiple steady states according to the advanced deficiency theory (deficiency of the network is three) for the given set of reaction rate constants taken with mass action kinetics as given in Figure 4.3. The numbers given in the middle are the normalized reaction rate constants.

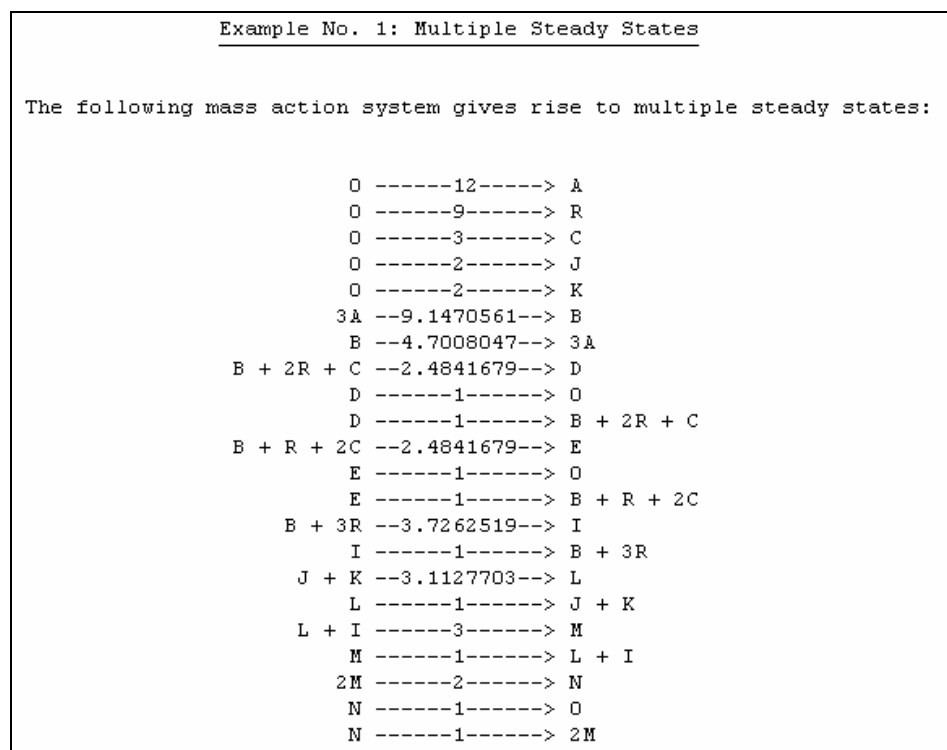


Figure 4.3. Rate constants of the FAS-mediated reaction network

The reaction network has a capacity for multiple steady states means that, there are rate constants that give rise to two or more positive (stoichiometrically compatible) steady states. CRNT also outputs a set steady state concentrations consistent with the network for the given reaction rate constants, and are given in Figure 4.4.

<u>Steady State No. 1</u>	<u>Species</u>	<u>Steady State No. 2</u>
0.84257549	A	1.1759088
1.3700988	R	0.70343222
1.3700988	C	0.70343222
0.70343222	J	1.3700988
1.3700988	K	0.70343222
0.31303528	B	2.3130352
1	D	1
1	E	1
1	I	1
1	L	1
1	M	1
1	N	1

Figure 4.4. Steady state concentrations for the FAS-mediated reaction network

The extrinsic signal (input to the FAS module), which is transmitted into the cell, provides the onset of sequence reactions causing apoptosis by forming DISC complex, which in turn activates caspase-8. Because of this, DISC can be referred to as the output of the FAS module. However, in Figure 4.4, it can be observed that the concentration of DISC (Species N) is one for both steady states. Therefore, the amount of DISC complex that will be present in the cell will be same in the steady state without depending on the initial conditions of the cell. Consequently, this module does not represent the bistable character of the apoptosis model.

4.1.2. Caspase-9 Activation Module

4.1.2.1. Caspase-9 Activation Module In the Presence of HSP70. Bistability analysis in different modules inside the mitochondria-dependent apoptosis module shows that caspase-9 activation module given in Figure 4.5 is a critical module to represent the bistable character of the apoptotic pathway.

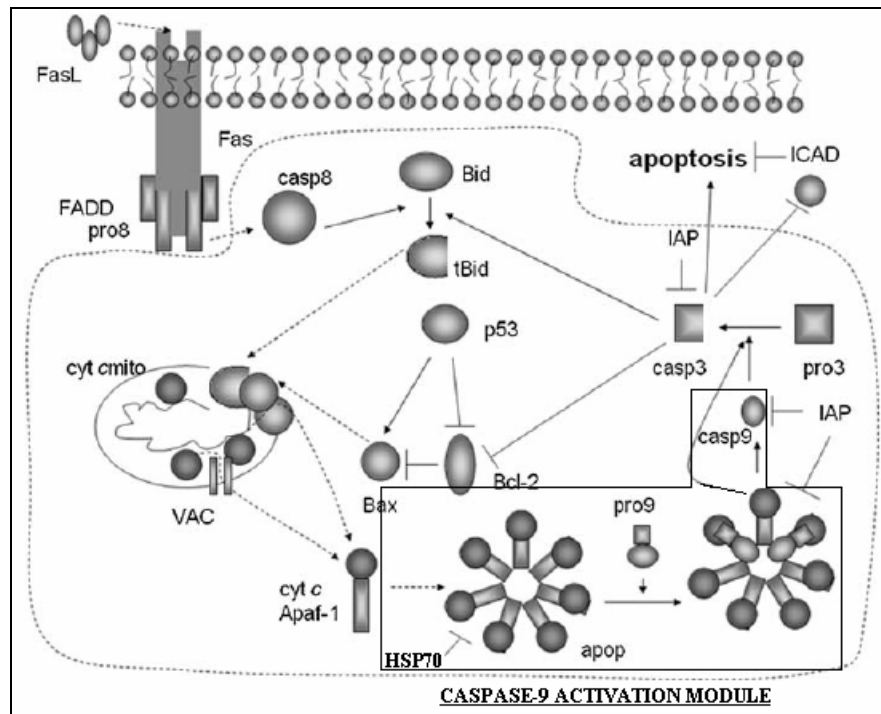


Figure 4.5. The Caspase-9 activation module adapted from Bagci *et al.* (2006)

Each component in the caspase-9 activation module is represented by a letter for simplicity in order to define them in CRNT and is given in Table 4.3.

Table 4.3. Representation of the species and complexes in the caspase-9 activation module

$\text{apop} \rightarrow A$	$\text{apop} \cdot (\text{pro9})_2 \rightarrow D$	$\text{casp9} \rightarrow G$
$\text{pro9} \rightarrow B$	$\text{apop} \cdot (\text{casp9})_2 \rightarrow E$	$\text{HSP70} \rightarrow H$
$\text{apop} \cdot \text{pro9} \rightarrow C$	$\text{apop} \cdot \text{casp9} \rightarrow F$	$\text{apop} \cdot \text{HSP70} \rightarrow I$

The reactions of the caspase-9 module are given in Table 4.4. Formation of procaspase-9/apoptosome complex is required for the cleavage and the activation of caspase-9. However, HSP70, the heat shock protein acts as an inhibitor that prevents the binding of procaspase-9 to apoptosome (Beere *et al.*, 2000). Also, both $\text{apop} \cdot (\text{casp9})_2$ holoenzyme and caspase-9 play a role in the proceeding steps in the apoptotic pathway by promoting the activation of executioner caspase-3. In this simulation, for simplicity it is assumed that two procaspase-9 bind to apoptosome (Bagci *et al.*, 2006), although up to seven procaspase-9 can theoretically bind to apoptosome (Zou *et al.* 1999).

Table 4.4. Representation of the reactions in the caspase-9 activation module

$0 \Rightarrow \text{apop}$	$0 \Rightarrow A$
$0 \Rightarrow \text{pro9}$	$0 \Rightarrow B$
$0 \Rightarrow \text{HSP70}$	$0 \Rightarrow H$
$\text{apop} + \text{HSP70} \Leftrightarrow \text{apop.HSP70}$	$A + H \Leftrightarrow I$
$\text{apop} + \text{pro9} \Leftrightarrow \text{apop.pro9}$	$A + B \Leftrightarrow C$
$\text{apop.pro9} + \text{pro9} \Leftrightarrow \text{apop.(pro9)}_2$	$C + B \Leftrightarrow D$
$\text{apop.(pro9)}_2 \Rightarrow \text{apop.(casp9)}_2$	$D \Rightarrow E$
$\text{apop.(casp9)}_2 \Leftrightarrow \text{apop.casp9} + \text{casp9}$	$E \Leftrightarrow F + G$
$\text{apop.casp9} \Leftrightarrow \text{apop} + \text{casp9}$	$F \Leftrightarrow A + G$
$\text{apop.HSP70} \Rightarrow 0$	$I \Rightarrow 0$
$\text{casp9} \Rightarrow 0$	$G \Rightarrow 0$

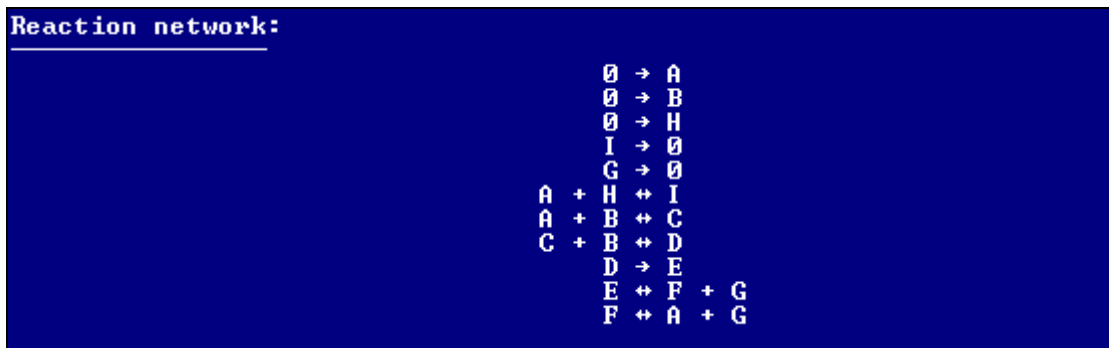


Figure 4.6. Reaction network of the caspase-9 activation module

When reactions of the caspase-9 activation module are entered into the CRNT program, firstly, Figure 4.6 appears as an output in a rearranged form. Then the following conclusion is made by the program:

“Taken with mass action kinetics, the network above does have the capacity for multiple steady states and for a degenerate steady state. That is, there are rate constants that give rise to two or more positive (stoichiometrically compatible) steady states”. Also, the program provides with the normalized reaction rate constants which will give rise to

multiple steady states and are given in Figure 4.7 and a set of normalized steady state concentrations consistent with the network for the given reaction rate constants and is shown in Figure 4.8.

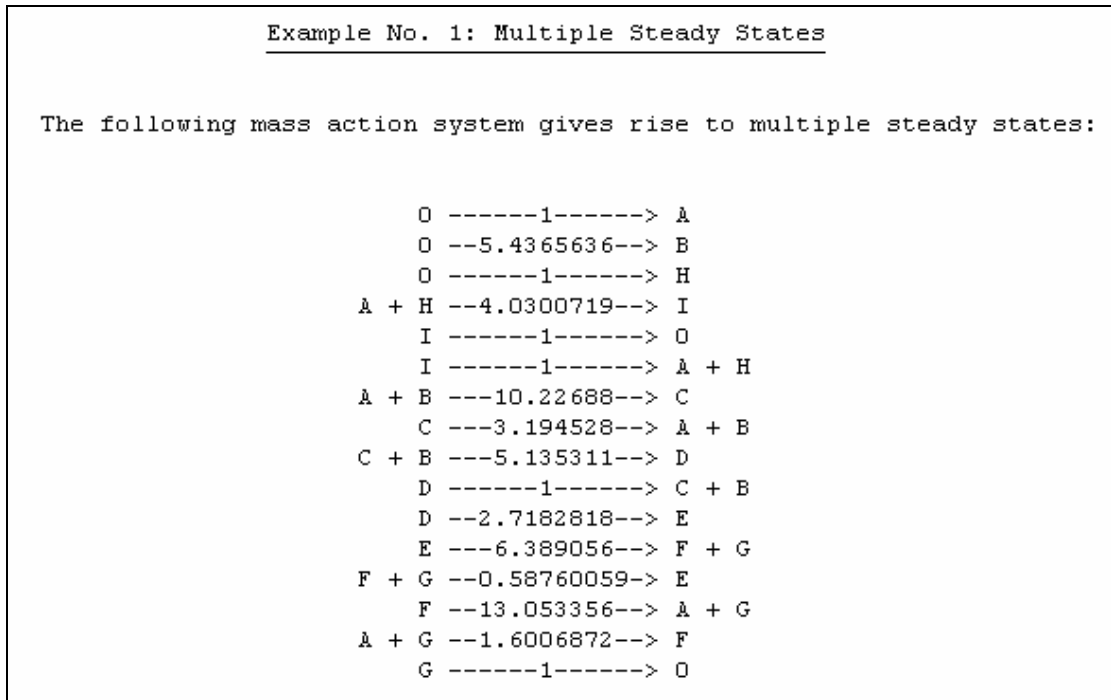


Figure 4.7. Rate constants of the reaction network of the caspase-9 activation module

<u>Steady State No. 1</u>	<u>Species</u>	<u>Steady State No. 2</u>
0.15718708	A	3.157187
2.3130352	B	0.31303528
0.31303528	C	2.3130352
1	D	1
0.5819767	E	1.5819767
0.31303528	F	2.3130352
5.4365636	G	5.4365636
3.157187	H	0.15718708
1	I	1

Figure 4.8. Steady state concentrations for the caspase-9 activation module reaction network

The outputs of this module, apop.(casp9)₂ holoenzyme (E) and caspase-9 (G) are crucial for cleavage of procaspase-3 and hence activation of caspase-3. The steady state concentration of caspase-9 is seen to be independent of the initial protein concentration. (5.44 in both steady states) whereas the steady state concentration of apop.(casp9)₂ is

dependent (0.58 in steady state I and 1.58 in steady state II). Hence, it can be inferred that this protein may be responsible for the bistable character of the mitochondria-dependent apoptotic pathway.

These steady states are also confirmed when XPPAUT is used. When it is desired to reach the steady state concentration in steady state number 1, the following procedure is used. If the concentration of a species is less than same species steady state concentration at steady state number 2, then a lower value is assigned as an initial value and conversely if higher, then a higher value is assigned. Using XPPAUT, the ODEs arising from mass action kinetics are integrated with these initial conditions and then the final concentration values are checked to see if they converge to those given by CRNT.

4.1.2.2. Caspase-9 Activation Module in the Absence of HSP70. It is expected that bistability in a module is the result of the inhibitory effect of a protein and may cause cell survival depending on the initial conditions of the cell. When the heat shock protein, HSP70, with the apoptosome is discarded from the sequence of reactions in the pathway as shown in Figure 4.9 and analyzed, deficiency of the reaction network calculated by CRNT reduces to one, and the network is analyzed by using Deficiency One Theory. Note that with the inhibitor HSP70 deficiency of the network is two. According to Deficiency One Theory, the corresponding differential equations cannot admit a steady state at which all species concentrations are positive, nor can the differential equations admit a cyclic composition trajectory that passes through a composition for which all species concentrations are positive for arbitrary kinetics.

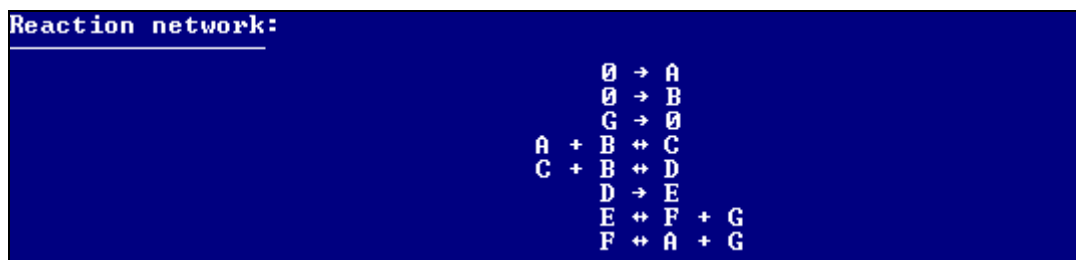


Figure 4.9. Reaction network of the caspase-9 activation module in the absence of HSP70

As is expected, multistationary behavior in the module is lost in the absence of HSP70. This situation can be explained by the inhibitory effect of HSP70 protein that causes a lower caspase-9 concentration, which in turn causes low caspase-3 concentration and hence a possible cell survival. Therefore, since caspase-9 is activated as a result of the interaction of apoptosome and procaspase-9 (cleavage of procaspase-9 and activation of caspase-9), the presence of HSP70 inhibitor renders the chemical reaction network to have capacity for multiequilibria and the absence causes monostability. It is concluded that inhibitors such as HSP70 are critical for the bistable character of the apoptotic pathway.

4.2. Bistability Analysis In Model 2

In order to investigate the bistability in model 2, the pathway involving Nitric Oxide (NO) effects is separated into three modules (compartments). Basically, these modules are ONOO⁻ module, N₂O₃ module, and FeL_nNO module. Modules are constructed in such a way that circularity is present in the modules i.e. reactive NO species (ONOO⁻, N₂O₃ and FeL_nNO) are produced due to the reactions of reactive species superoxide (O₂⁻), O₂ and non-heme iron compounds (FeL_n) respectively with NO and later NO is produced within the module. These modules are not independent from each other and contain some common reactions such as interactions with the antioxidant glutathione (GSH). GSH has important role in the cell, since it protects cells from toxins such as free radicals. GSH also modulates the concentrations of NO species (ONOO⁻, N₂O₃ and FeL_nNO) in the cell. GSH is converted by these reactions to GSNO, which is then converted to GSSG and finally back to GSH. Hence, NO modules contain two feedback loops: NO and GSH loops. Also, Bagci *et al.* (2008) shows that GSH plays critical role for regulating NO species concentration. The created modules of the NO pathway are given in the Figure 4.10. The set of reactions containing NO effects on the pathway is taken from Bagci *et al.* (2008) and is given in Table 4.5.

Table 4.5. The set of reactions containing NO effects on the apoptotic pathway (Bagci *et al.*, 2008)

Description of the reaction/interaction	
ONOO⁻ Production	
$SOD + O_2^- + H^+ \Rightarrow SOD + 1/2 O_2 + 1/2 H_2O_2$	$r_{5NO} = k_{5NO}[SOD][O_2^-]$
$O_2^- + NO \Rightarrow ONOO^-$	$r_{4NO} = k_{4NO}[NO][O_2^-]$
$ONOO^- + GSH \Rightarrow GSNO + products$	$r_{6NO} = k_{6NO}[ONOO^-][GSH]$
$ONOO^- + GPX \Rightarrow GPX + products$	$r_{7NO} = k_{7NO}[ONOO^-][GPX]$
$ONOO^- + CO_2 \Rightarrow products$	$r_{8NO} = k_{8NO}[ONOO^-][CO_2]$
$ONOO^- + cyt\ c \Rightarrow cyt\ c + products$	$r_{9NO} = k_{9NO}[ONOO^-][cyt\ c]$
N₂O₃ Production	
$2NO + O_2 \Rightarrow 2NO_2$	$r_{12aNO} = k_{12aNO}[NO]^2[O_2]$
$NO_2 + NO \Leftrightarrow N_2O_3$	$r_{12bNO}^+ = k_{12bNO}^+[NO_2][NO]$ $r_{12bNO}^- = k_{12bNO}^-[N_2O_3]$
$N_2O_3 + GSH \Rightarrow GSNO + NO_2^- + H^+$	$r_{11NO} = k_{11NO}[N_2O_3][GSH]$
$N_2O_3 + H_2O \Rightarrow products$	$r_{13NO} = k_{13NO}[N_2O_3]$
FeL_nNO Production	
$FeL_n + NO \Rightarrow FeL_nNO$	$r_{16NO} = k_{16NO}[FeL_n][NO]$
$FeL_nNO + GSH \Rightarrow GSNO + FeL_n$	$r_{17NO} = k_{17NO}[FeL_nNO][GSH]$
Common Reactions	
$0 \Rightarrow NO$	$r_{1NO} = k_{1NO}$
$0 \Rightarrow O_2^-$	$r_{2NO} = k_{2NO}$
$0 \Rightarrow GSH$	$r_{3NO} = k_{3NO}$
$CcOx + NO \Rightarrow CcOx.NO$	$r_{15NO} = k_{15NO}[CcOx][NO]$
$GSH + O_2^- \Rightarrow 1/2 GSSG + products$	$r_{17bNO} = k_{17bNO}[GSH][O_2^-]$
$2GSNO + O_2^- + H_2O \Rightarrow GSSG + products$	$r_{10NO} = k_{10NO}[GSNO]^2[O_2^-]$
$Cu^+ GSNO \Rightarrow 1/2 GSSG + NO$	$r_{14NO} = k_{14NO}[GSNO]$
$GSSG + NADPH + H^+ \Rightarrow NADP^+ + 2GSH$	$r_m = V_m[GSSG]/(K_m + [GSSG])$

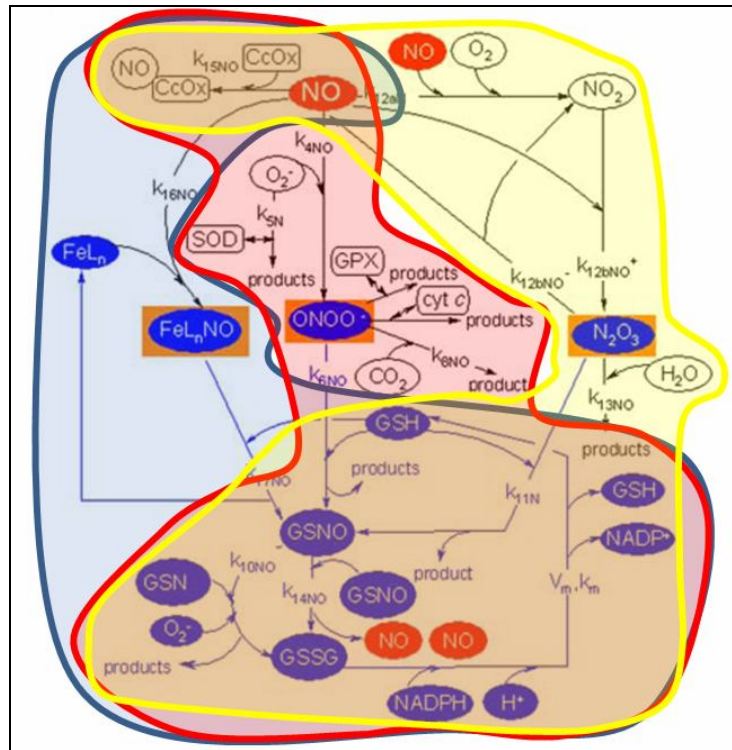


Figure 4.10. Modules of the NO Pathway adapted from Bagci *et al.* (2008) (ONOO⁻ module: Red, N₂O₃ module: Yellow, and FeL_nNO module: Blue)

4.2.1. Bistability Analysis in ONOO⁻ Module

ONOO⁻ is produced by the reaction of highly reactive O₂⁻ (superoxide) with NO. The stress due to highly oxidative effect of O₂⁻ and ONOO⁻ is reduced by the anti-oxidizing effect of GSH. ONOO⁻ plays pro-apoptotic effect in apoptosis by promoting the cytochrome *c* (cyt *c*) release from mitochondria via acting on mitochondrial permeability transition pore complex (MPTP complex). The interactions in the ONOO⁻ module are indicated by red color in the Figure 4.11. Some side reactions in the Figure 4.11 are discarded due to limitations of CRNT program. The set of reactions used in the simulation is given in the Table 4.6. Note that some modifications are made on the reactions taken from Bagci *et al.* (2008). The reactions are written in such a way that only those reactants affecting the rate of the given reaction are considered and the components which are referred as “products” in Bagci *et al.* (2008) are excluded from the reaction equation given in Table 4.6. For example, since water is not included in the rate equation $r_{10NO} = k_{10NO} [GSNO]^2 [O_2^-]$, the reaction given by Bagci *et al.*, (2008) in Table 4.5

$2GSNO + O_2^- + H_2O \Rightarrow GSSG + products$ is represented as $2GSNO + O_2^- \Rightarrow GSSG$ in Table 4.6.

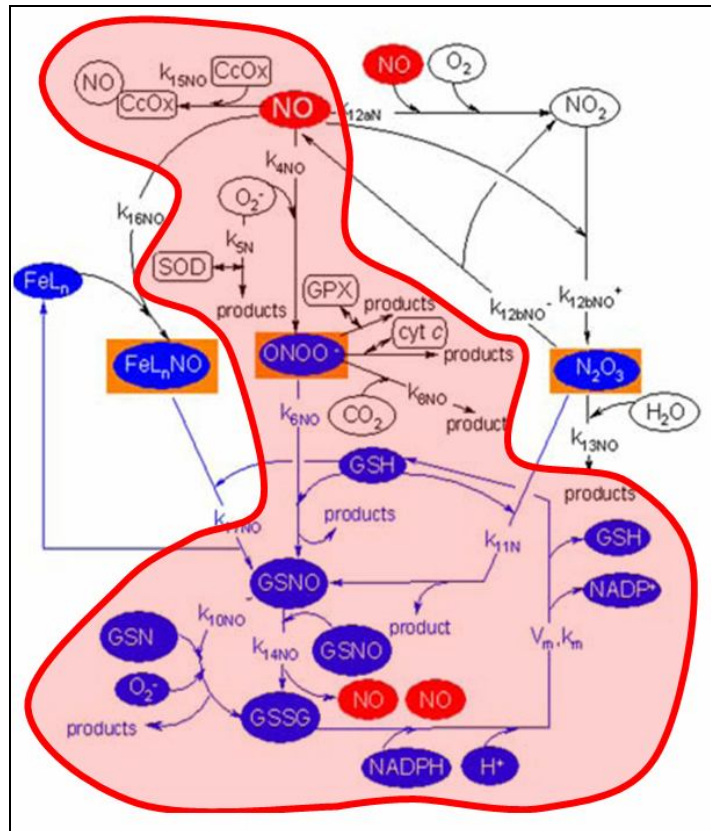


Figure 4.11. $ONOO^-$ module reaction pathway adapted from Bagci *et al.* (2008)

Table 4.6. Reactions of $ONOO^-$ module and their letter representations

$0 \Rightarrow NO$	$0 \Rightarrow A$
$0 \Rightarrow O_2^-$	$0 \Rightarrow B$
$O_2^- + NO \Rightarrow ONOO^-$	$B + A \Rightarrow F$
$ONOO^- + GSH \Rightarrow GSNO$	$F + C \Rightarrow E$
$2GSNO \Rightarrow GSSG + 2NO$	$2E \Rightarrow D + 2A$
$2GSNO + O_2^- \Rightarrow GSSG$	$2E + B \Rightarrow D$
$GSSG \Rightarrow 2GSH$	$D \Rightarrow 2C$
$2GSH + 2O_2^- \Rightarrow GSSG$	$2C + 2B \Rightarrow D$

CRNT analysis shows that the ONOO⁻ module does have capacity for multiple steady states for the following mass action system given in Table 4.6 according to advanced deficiency theorem, which gives a deficiency of three for this network.

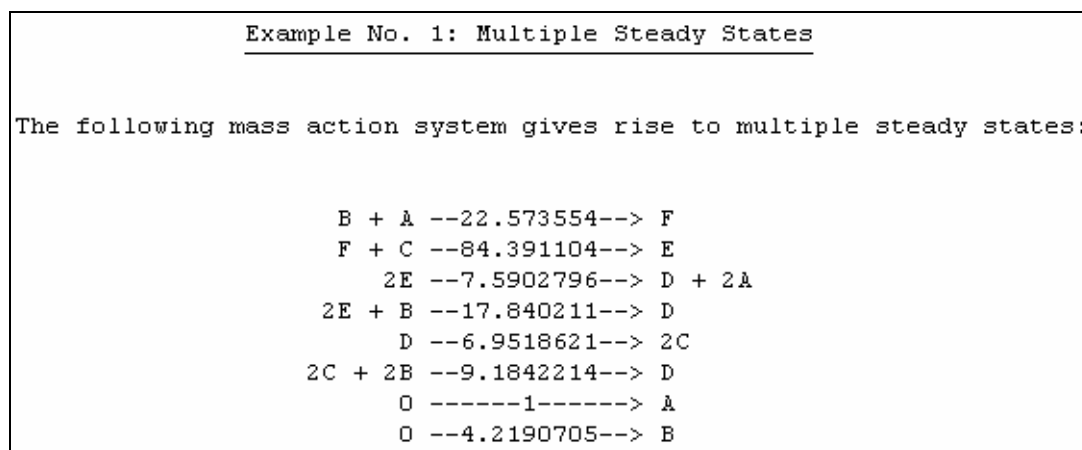


Figure 4.12. Normalized reaction rate constants given by CRNT for ONOO⁻ module

By using the reaction rate constants given by CRNT which are presented in Figure 4.12, the steady states given in Figure 4.13 are obtained.

<u>Steady State No. 1</u>	<u>Species</u>	<u>Steady State No. 2</u>
1.0523956	A	5.2395 E-2
0.15651764	B	1.1565176
4.1866 E-2	C	0.30935385
0.26748736	D	0.26748736
0.42315877	E	0.15567141
1.0523956	F	5.2395 E-2

Figure 4.13. Steady states obtained from CRNT analysis for ONOO⁻ module

Eigenvalues of steady state I show that state is an unstable state, since one of its eigenvalue has positive real part as shown in Figure 4.14. Unstable steady states cannot be reproduced by XPPAUT, as the program output of some concentrations diverges.

```

Eigenvalues for Steady State No. 1

-229720.35
-78419.56
-65420.47
-906.98362
696.16095

Steady State No. 1 is unstable.

```

Figure 4.14. Eigenvalues of steady state I given for ONOO⁻ module

On the other hand, asymptotically stable state (steady state II) can be obtained using ODE solver XPPAUT. Figure 4.15 shows that all eigenvalues of steady state II have negative real parts.

```

Eigenvalues for Steady State No. 2

(-85711.774) + i (28653.992)
(-85711.774) - i (28653.992)
-67096.604
-3277.1444
-16952.363

Steady State No. 2 is asymptotically stable.

```

Figure 4.15. Eigenvalues of steady state II given for ONOO⁻ module

In summary, the species of concern of this module is ONOO⁻ and has pro-apoptotic effect on apoptosis by increasing the cyt *c* release from mitochondria. The CRNT results show that ONOO⁻ module has bistable character. In steady state I, ONOO⁻ (F) has normalized steady state value of 1.05 and it is approximately 0.05 in steady state II as given in Figure 4.13. Therefore, depending on the initial conditions in the cell, cyt *c* release from mitochondria is high in one steady, but low in another state. This will affect the apoptosome formation, caspase-9 activation and hence executioner caspase-3 activation. Because of this, bistability in ONOO⁻ module is conjectured to be responsible for the bistable character of apoptotic pathway.

4.2.2. Bistability Analysis in N_2O_3 Module

N_2O_3 is produced in the apoptotic pathway in the presence of O_2 in the cell. Firstly, NO_2 is formed, which is followed by the reaction of this molecule with NO to produce the product N_2O_3 . N_2O_3 has anti-apoptotic effect in the apoptosis. It inhibits caspase-8, which provides the cleavage of pro-apoptotic Bid protein and the activation of tBid (truncated Bid). The interactions in the N_2O_3 module are shown by yellow color in Figure 4.16. Again, some side reactions in the N_2O_3 module are discarded because of the limitations in CRNT and the letter representations of the following reactions are used to analyze bistability in that module as given in Table 4.7.

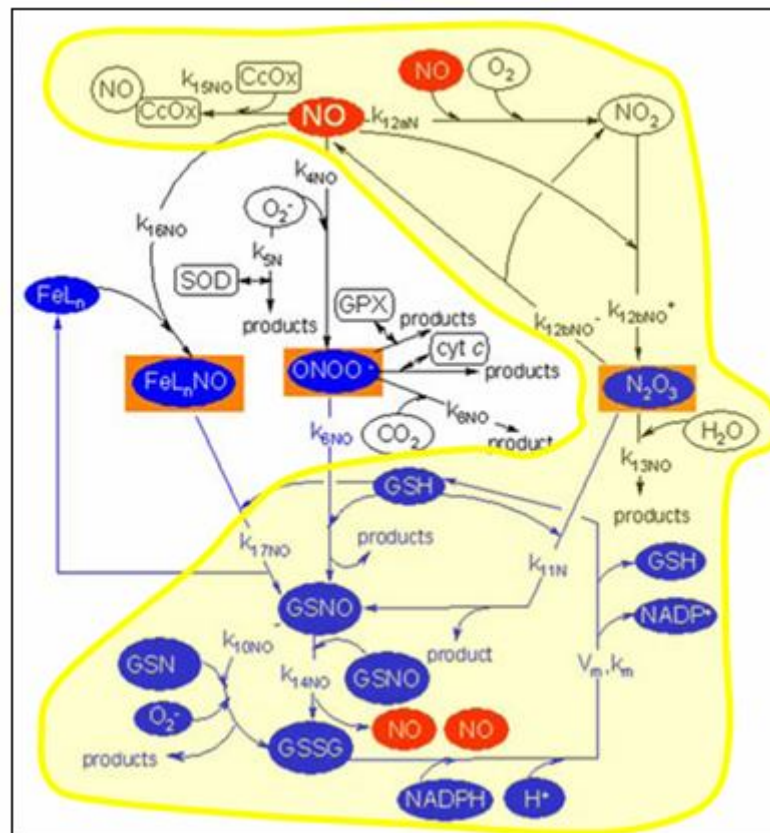


Figure 4.16. N_2O_3 module reaction pathway adapted from Bagci *et al.* (2008)

Table 4.7. Reactions of N_2O_3 module and their letter representations

$0 \Rightarrow NO$	$0 \Rightarrow A$
$0 \Rightarrow O_2^-$	$0 \Rightarrow B$
$2NO + O_2 \Rightarrow 2NO_2$	$2A + F \Rightarrow 2G$
$NO_2 + NO \Leftrightarrow N_2O_3$	$G + A \Leftrightarrow H$
$N_2O_3 + GSH \Rightarrow GSNO$	$H + C \Rightarrow E$
$2GSNO \Rightarrow GSSG + 2NO$	$2E \Rightarrow D + 2A$
$2GSNO + O_2^- \Rightarrow GSSG$	$2E + B \Rightarrow D$
$GSSG \Rightarrow 2GSH$	$D \Rightarrow 2C$
$2GSH + 2O_2^- \Rightarrow GSSG$	$2C + 2B \Rightarrow D$

According to CRNT analysis, the N_2O_3 module cannot admit multiple positive steady states no matter what positive value the reaction rate constants might have. Consequently, the N_2O_3 module does not have bistable character and cannot be responsible for the bistability of the apoptotic pathway.

4.2.3. Bistability Analysis in FeL_nNO Module

FeL_nNO is formed by the reaction of FeL_n with NO and has anti-apoptotic affect on the apoptotic pathway. It inhibits caspase-9 and executioner caspase-3, thereby preventing the cell death. The concentration of FeL_nNO is especially high in hepatocytes (Bagci *et al.*, 2008). The reaction pathway and interactions in the FeL_nNO module are shown in the Figure 4.17. The set of reactions in the FeL_nNO module after discarding some side reactions without importance are given in the Table 4.8 with their letter representations.

CRNT analysis has shown that FeL_nNO module also cannot admit multiple positive steady states no matter what positive value the reaction rate constants might have. Therefore, the FeL_nNO module has monostable character and cannot be responsible for the bistability of the apoptotic pathway.

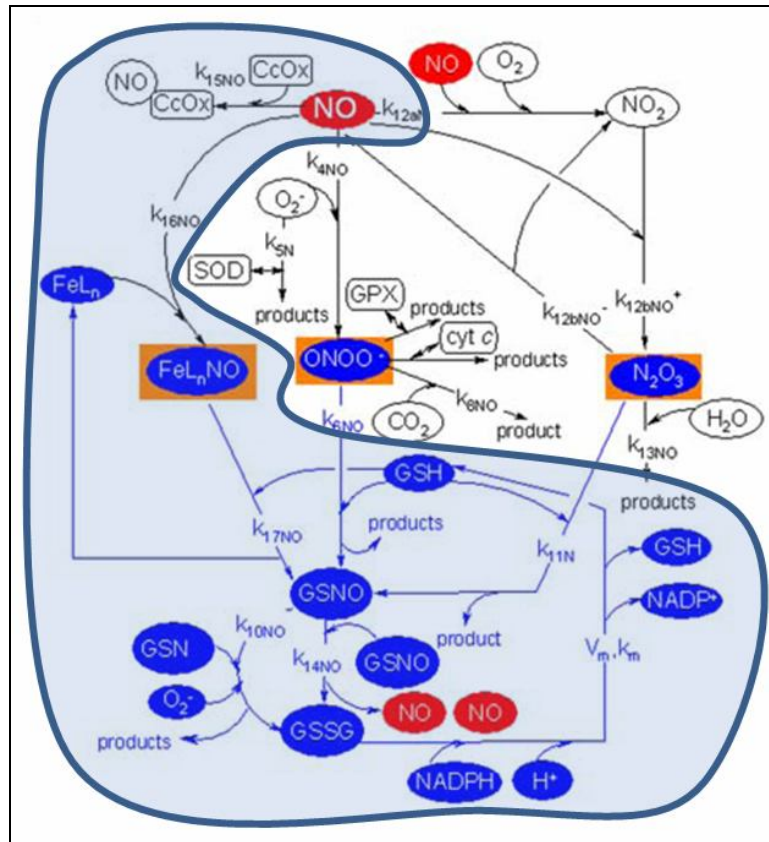


Figure 4.17. FeL_nNO module reaction pathway adapted from Bagci *et al.* (2008)

Table 4.8. Reactions of FeL_nNO module and their letter representations

$0 \Rightarrow NO$	$0 \Rightarrow A$
$0 \Rightarrow O_2^-$	$0 \Rightarrow B$
$FeL_n + NO \Rightarrow FeL_nNO$	$F + A \Rightarrow G$
$FeL_nNO + GSH \Rightarrow GSNO + FeL_n$	$G + C \Rightarrow E + F$
$2GSNO \Rightarrow GSSG + 2NO$	$2E \Rightarrow D + 2A$
$2GSNO + O_2^- \Rightarrow GSSG$	$2E + B \Rightarrow D$
$GSSG \Rightarrow 2GSH$	$D \Rightarrow 2C$
$2GSH + 2O_2^- \Rightarrow GSSG$	$2C + 2B \Rightarrow D$

In conclusion, among the selected three modules namely $ONOO^-$, N_2O_3 and FeL_nNO , only the $ONOO^-$ module does have capacity for multiequilibria whereas the other two do not. Therefore, model 2 is obtained around this module as explained in the next section.

4.3. Model Development

After carrying out bistability analysis on different modules, model 1 and model 2 are constructed by assuming that bistable character in a module will represent the bistable character of the whole model. To this end, first the steady state concentrations obtained by CRNT results are reproduced by the help of the ODE solver XPPAUT using the reaction rate constants given by CRNT. Then, these dimensionless rate constants are converted to biologically meaningful units. By adding the other reaction equations to the bistable module, model 1 and model 2 are then formed. Finally, model 1 (mitochondria-dependent apoptosis model) and model 2 (NO species effects on the apoptosis) are combined to constitute the overall model (model 3). The construction of model 3 may enable one to carry out analysis for different cell types and conditions such as investigations on the chemotherapy resistance.

4.3.1. Reproduction of Steady States by Using XPPAUT

The CRNT results given in Sections 4.1 and 4.2 show that the caspase-9 activation module in model 1 and the ONOO⁻ module in model 2 are critical for the bistable character of the mitochondria-dependent apoptosis model. Furthermore, CRNT results should be reproduced by the ODE solver XPPAUT. This will help to expand a bistable module to form model 1 or model 2 by the addition of the remaining reactions in the pathway, which are expressed in terms ordinary differential equations. For different initial conditions, differential equations of the caspase-9 activation module are integrated by XPPAUT. The final steady state values reached are given in Figure 4.18 and Figure 4.19 and are very close to those obtained from CRNT (Table 4.8).

Time	APOP	C9Z	APOPC9Z	APOPC9Z2	APOPC9A2
18000	0.1568525	2.316928	0.3125115	1	0.5818442
Time	APOPC9A	C9A	HSP70	APOPHSP	
18000	0.3127708	5.4366	3.163979	1	

Figure 4.18. Steady state I of caspase-9 activation module

The reaction rate constants obtained from by CRNT are also checked for the caspase-9 activation module to see whether they are biologically meaningful with the available reaction rate constants given in the literature. By this way, mitochondria-dependent apoptotic pathway is constructed.

Time	APOP	C9Z	APOPC9Z	APOPC9Z2	APOPC9A2
18000	3,174687	0,3120372	2,32045	1	1,587367

Time	APOPC9A	C9A	HSP70	APOPHSP
18000	2,323819	5,4366	0,1563234	1

Figure 4.19. Steady state II of caspase-9 activation module

The integration of the ordinary differential equations in ONOO^- module gives the following steady states shown in Figure 4.20 and Figure 4.21. The comparison of Figure 4.13 and Figures 4.20 and 4.21, shows that the asymptotically stable state obtained by CRNT analysis can be reproduced, while unstable state cannot. This is because, depending on the initial conditions, concentrations of the components in ONOO^- module can diverge to very high values as shown in Figure 4.21. However, this is not a reasonable situation within the cell. High concentration of ONOO^- may give harm to cell due to high oxidative stress besides its pro-apoptotic effects and may cause necrosis.

GSH	NO	O2M	ONOOM	GSNO
0,3093694	0,052398	1,156453	0,05239356	0,1556767

Figure 4.20. Asymptotically stable steady state for ONOO^- module

GSH	NO	O2M	ONOOM	GSNO
1,101868e-06	21480,52	8,701216e-06	38472,39	0,4854374

Figure 4.21. Unstable state for ONOO^- module

4.3.2. Biological Plausibility of the CRNT Rate Constants

As mentioned in Section 3, CRNT is a very useful program that predicts the multistationarity of a given reaction network from its network structure. When capacity for multiplicity is determined for a given chemical reaction network, the program produces reaction rate constants as an output that satisfy the bistability condition. This toolbox can also be used for bistability analysis in biological systems. However, the reaction rate constants given by CRNT should be checked and compared with the parameter range obtained from experimental studies available in the literature. The reaction rate constants given by CRNT are normalized reaction rate constants. Therefore, order of magnitude of molarity unit of concentrations can be assigned arbitrarily to these rate constants. It should be noted that time unit used in reaction rate constant is selected in terms of seconds for simplicity.

Table 4.9. Comparison of reaction rate constants given by CRNT and proposed by Bagci *et al.* (2008) for caspase-9 activation module

Reaction	Rate Constant by CRNT (dimensionless)	Rate Constant by Bagci <i>et al.</i> (2008) (in terms of μM)
$0 \Rightarrow \text{apop}$	$\text{Ap}_f=1$	-
$0 \Rightarrow \text{pro9}$	$\text{pro9}_f=5.44$	$\text{pro9}_f=0.0003$
$0 \Rightarrow \text{HSP70}$	$\text{HSP70}_f=1$	-
$\text{apop} + \text{HSP70} \Leftrightarrow \text{apop.HSP70}$	$k_{15p}=4.03$ $k_{15m}=1.00$	-
$\text{apop} + \text{pro9} \Leftrightarrow \text{apop.pro9}$	$k_{2p}=10.23$ $k_{2m}=3.19$	$k_{2p}=10$ $k_{2m}=0.5$
$\text{apop.pro9} + \text{pro9} \Leftrightarrow \text{apop.(pro9)}_2$	$k_{3p}=5.14$ $k_{3m}=1.00$	$k_{3p}=10$ $k_{3m}=0.5$
$\text{apop.(pro9)}_2 \Rightarrow \text{apop.(casp9)}_2$	$k_{3f}=2.72$	$k_{3f}=0.1$
$\text{apop.(casp9)}_2 \Leftrightarrow \text{apop.casp9} + \text{casp9}$	$k_{4p}=6.39$ $k_{4m}=0.59$	$k_{4p}=5$ $k_{4m}=0.5$
$\text{apop.casp9} \Leftrightarrow \text{apop} + \text{casp9}$	$k_{4bp}=13.05$ $k_{4bm}=1.60$	$k_{4bp}=5$ $k_{4bm}=0.5$
$\text{apop.HSP70} \Rightarrow 0$	$\text{apop.HSP70}_{\text{deg}}=1$	-
$\text{casp9} \Rightarrow 0$	$\text{p9}_{\text{deg}}=1$	$\text{p9}_{\text{deg}}=0.006$

In order to assign the magnitude of the molarity unit, the reaction rate constants given by CRNT are compared with the literature values as shown in Table 4.9 for caspase-9 activation module. It is seen that there is not significant difference with the parameter values used by Bagci *et al.* (2008) except the formation and degradation rates, which are taken from Bagci *et al.* (2008). Consequently, the magnitude of the reaction rate constants is selected in terms of μM (10^{-6} M). The reaction rate constants used for caspase-9 activation module simulation is tabulated in Table 4.10.

Table 4.10. Reaction rate constants used for caspase-9 activation module simulation

Reaction	Reaction Rate Constant (in terms of μM)
$0 \Rightarrow \text{apop}$	$\text{Ap}_f=1$
$0 \Rightarrow \text{pro9}$	$\text{pro9}_f=0.0003$
$0 \Rightarrow \text{HSP70}$	$\text{HSP70}_f=1$
$\text{apop} + \text{HSP70} \Leftrightarrow \text{apop.HSP70}$	$k_{15p}=4.03$ $k_{15m}=1.00$
$\text{apop} + \text{pro9} \Leftrightarrow \text{apop.pro9}$	$k_{2p}=10.23$ $k_{2m}=3.19$
$\text{apop.pro9} + \text{pro9} \Leftrightarrow \text{apop.(pro9)}_2$	$k_{3p}=5.14$ $k_{3m}=1.00$
$\text{apop.(pro9)}_2 \Rightarrow \text{apop.(casp9)}_2$	$k_{3f}=2.72$
$\text{apop.(casp9)}_2 \Leftrightarrow \text{apop.casp9} + \text{casp9}$	$k_{4p}=6.39$ $k_{4m}=0.59$
$\text{apop.casp9} \Leftrightarrow \text{apop} + \text{casp9}$	$k_{4bp}=13.05$ $k_{4bm}=1.60$
$\text{apop.HSP70} \Rightarrow 0$	$\text{apop.HSP70}_{\text{deg}}=1$
$\text{casp9} \Rightarrow 0$	$\text{p9}_{\text{deg}}=0.006$

Same procedure is also followed for bistable ONOO⁻ module. The comparison of reaction rate constants given by CRNT and Bagci *et al.* (2008) is tabulated in Table 4.11.

Table 4.11. Comparison of reaction rate constants given by CRNT and proposed by Bagci *et al.* (2008) for ONOO⁻ module

Reaction	Rate Constant by CRNT (dimensionless)	Rate Constant by Bagci <i>et al.</i> (2008) (in terms of μM)
$0 \Rightarrow NO$	$k_{1NO}=1.00$	$k_{1NO}=1.00$
$0 \Rightarrow O_2^-$	$k_{2NO}=4.22$	$k_{2NO}=0.1$
$O_2^- + NO \Rightarrow ONOO^-$	$k_{4NO}=22.57$	$k_{4NO}=6700$
$ONOO^- + GSH \Rightarrow GSNO$	$k_{6NO}=84.39$	$k_{6NO}=0.00135$
$2GSNO \Rightarrow GSSG + 2NO$	$k_{14NO}=7.59$	$k_{14NO}=0.0002$
$2GSNO + O_2^- \Rightarrow GSSG$	$k_{10NO}=17.84$	$k_{10NO}=0.0006$
$GSSG \Rightarrow 2GSH$	$k_m=6.95$	$V_m=320, K_m=50$
$2GSH + 2O_2^- \Rightarrow GSSG$	$k_{17NOb}=9.18$	$k_{17NOb}=0.0002$

As it can be observed from the Table 4.11, there are very significant differences between the reaction rate constants given by CRNT and those used by Bagci *et al.* (2008). Because of this, order of magnitude of molarity is assigned as mM (10^{-3} M) as this yields parameter values which are more close to experimental values given in the literature. To this end, the concentration values of the components given by that program are multiplied by 1000 to convert the units to μM as it is used by Bagci *et al.* (2008).

It is also necessary to convert rate of reactions as calculated from the reaction rate constants given by CRNT from mM/s to μM/s by changing the rate constants for different order of reactions in the following manner.

Zero-Order Reaction: Unit of the reaction rate constant => mM /s

1st Order Reaction: Unit of the reaction rate constant => 1/s

2nd Order Reaction: Unit of the reaction rate constant => 1/mM.s

3rd Order Reaction: Unit of the reaction rate constant => 1/(mM)².s

Therefore, to convert the units given by CRNT to that of used by Bagci *et al.* (2008) (μM), the reaction rate constants should be multiplied by 10^3 for the zero order reactions, by 10^{-3} for the 2nd order reactions, by 10^{-6} for the 3rd order reactions, and by 10^{-9} for the 4th order reactions. Since, reaction rate constants of the 1st order reactions do not contain concentration terms, no conversion factor is needed for these reactions.

After carrying out the calculations summarized above, the reaction rate constants in Table 4.12 are obtained and compared with Bagci *et al.* (2008) to check if they are biologically plausible figures. If the reaction rate constants given by the CRNT are close to that used by Bagci *et al.* (2008) (less than 100 times), they are accepted as reasonable and not changed (reactions (4), (5) and (6) in Table 4.12). On the other hand, the reaction rate constants proposed by Bagci *et al.* (2008) and Hu *et al.* (2006) are used instead of those given by CRNT for reactions (3), (7) and (8) in Table 4.11, when their relative ratios are greater than 100. When the ODEs are integrated using XPPAUT, it is observed that bistable states are not lost, if these corrected reaction rate constants are used. It should be also noted that the bistable character of the module is strongly dependent on the formation rate constants of NO and O_2^- (reactions (1) and (2)). However, they are not changed so as to preserve the bistability although their values are very high in comparison to those given in the literature. Finally, reaction rate constants used in ONOO⁻ module are tabulated in Table 4.13.

After the biologically reasonable rate constants that give rise to two steady state conditions depending on the initial concentrations in the cell are found, rate expressions of the other reactions in the apoptotic pathway are added to form model 1 and model 2.

Table 4.12. Comparison of reaction rate constants given by CRNT and proposed by Bagci *et al.* (2008) for ONOO⁻ module after unit conversion

Reaction	Rate Constant by CRNT (in terms of μM)	Rate Constant by Bagci <i>et al.</i> (2008) (in terms of μM)	Approximate Relative Ratios
$0 \Rightarrow \text{NO}$ (1)	$k_{1\text{NO}}=1000$	$k_{1\text{NO}}=1.00$	1,000
$0 \Rightarrow \text{O}_2^-$ (2)	$k_{2\text{NO}}=4219$	$k_{2\text{NO}}=0.1$	42,190
$\text{O}_2^- + \text{NO} \Rightarrow \text{ONOO}^-$ (3)	$k_{4\text{NO}}=22.57 \times 10^{-3}$	$k_{4\text{NO}}=6700$	300,000
$\text{ONOO}^- + \text{GSH} \Rightarrow \text{GSNO}$ (4)	$k_{6\text{NO}}=84.39 \times 10^{-3}$	$k_{6\text{NO}}=0.00135$	62
$2\text{GSNO} \Rightarrow \text{GSSG} + 2\text{NO}$ (5)	$k_{14\text{NO}}=7.59 \times 10^{-3}$	$k_{14\text{NO}}=0.0002$	38
$2\text{GSNO} + \text{O}_2^- \Rightarrow \text{GSSG}$ (6)	$k_{10\text{NO}}=17.84 \times 10^{-6}$	$k_{10\text{NO}}=0.0006$	34
$\text{GSSG} \Rightarrow 2\text{GSH}$ (7)	$k_m=6.95$	$V_m=320,$ $K_m=50$	-
$2\text{GSH} + 2\text{O}_2^- \Rightarrow \text{GSSG}$ (8)	$k_{17\text{NO}b}=9.18 \times 10^{-9}$	$k_{17\text{NO}b}=0.0002$	22,000

Table 4.13. Reaction rate constants used for ONOO⁻ module simulation

Reaction	Reaction Rate Constant (in terms of μM)
$0 \Rightarrow \text{NO}$ (1)	$k_{1\text{NO}}=1000$
$0 \Rightarrow \text{O}_2^-$ (2)	$k_{2\text{NO}}=4219$
$\text{O}_2^- + \text{NO} \Rightarrow \text{ONOO}^-$ (3)	$k_{4\text{NO}}=6700$
$\text{ONOO}^- + \text{GSH} \Rightarrow \text{GSNO}$ (4)	$k_{6\text{NO}}=84.39 \times 10^{-3}$
$2\text{GSNO} \Rightarrow \text{GSSG} + 2\text{NO}$ (5)	$k_{14\text{NO}}=7.59 \times 10^{-3}$
$2\text{GSNO} + \text{O}_2^- \Rightarrow \text{GSSG}$ (6)	$k_{10\text{NO}}=17.84 \times 10^{-6}$
$\text{GSSG} \Rightarrow 2\text{GSH}$ (7)	$k_m=6.95$
$2\text{GSH} + 2\text{O}_2^- \Rightarrow \text{GSSG}$ (8)	$k_{17\text{NO}b}=0.0002$

4.3.3. Formation of Models

After determining bistable modules for both models with biologically reasonable rate constants, the models are completed by adding the rate expressions of remaining reactions in the apoptotic pathway. As explained in the previous sections, the rate constants obtained from CRNT are modified when necessary and then used as the parameter values of the ODEs obtained from mass action kinetics. This way, bistable apoptosis model containing NO effects in the absence of cooperativity is constructed. The mathematical expressions of model 1 (mitochondria-dependent apoptosis model in the absence of NO effects), model 2 (model of NO effects on the apoptotic pathway) and model 3 (overall model combining model 1 and model 2) are given in Table 4.14, Table 4.15 and Table 4.16 respectively.

The reaction expressions and their corresponding rate constants, net formation rate of a species due to a reaction (defined as forward minus reverse reaction rate) which is denoted by J , initial concentrations of components, and the parameters used in model 1, model 2 and model 3 are given in the Appendix A.

For example, in Table 4.14 for equation index (1), J_{1b} means the following: for model 1 in Table A.1 of Appendix A.1, the net formation rate for reaction index (1b) is $J_{1b} = r_{1bp} - r_{1bm}$ where the subscript in r_{1bp} denotes forward (plus) reaction rate and r_{1bm} denotes reverse (minus) reaction rate of reaction (1b).

Table 4.14. Mathematical expression of model 1 in terms of ordinary differential equations

Equation Index	Ordinary Differential Equations (Model 1)
(1)	$d[\text{Apop}]/dt = J_{1b} - J_2 + J_{4b} - J_{15} + j_{\text{Apop}}$
(2)	$d[\text{c9z}]/dt = -J_2 - J_3 + J_{p9}$
(3)	$d[\text{Apopc9z}]/dt = J_2 - J_3$
(4)	$d[\text{Apopc9z2}]/dt = J_3 - J_{3f}$
(5)	$d[\text{Apopc9a2}]/dt = J_{3f} - J_4 - J_{5c} - J_{6b} + J_{6bf}$
(6)	$d[\text{Apopc9a}]/dt = J_4 - J_{4b} - J_{5b}$
(7)	$d[\text{c9a}]/dt = J_4 + J_{4b} - J_5 - J_6 + J_{6f} + j_{p9a}$
(8)	$d[\text{c3a}]/dt = J_{6f} + J_{6bf} - J_7 - J_8 + J_{8f} - J_9 + J_{9f} - \mu \times c3a$
(9)	$d[\text{HSP70}]/dt = -J_{15} + j_{\text{Hsp}}$
(10)	$d[\text{ApopHSP}]/dt = J_{15} + j_{\text{Aph}}$
(11)	$d[\text{Cc}]/dt = j_{14} - J_1 - \mu \times \text{Cc} + \text{MPTP} \times \text{Cc}_{\text{mito}}$
(12)	$d[\text{Ap}]/dt = -J_1 + J_{\text{Ap}}$
(13)	$d[\text{CcAp}]/dt = J_1 - 7 \times J_{1b}$
(14)	$d[\text{IAP}]/dt = -J_5 - J_{5b} - J_{5c} - J_7 + J_{\text{IAP}}$
(15)	$d[\text{IAP9}]/dt = J_5$
(16)	$d[\text{IAPA9}]/dt = J_{5b}$
(17)	$d[\text{IAPA29}]/dt = J_{5c}$
(18)	$d[\text{c3z}]/dt = -J_6 - J_{6b} + J_{p3} - 10 \times \text{nop} \times c3z$
(19)	$d[\text{c93}]/dt = J_6 - J_{6f}$
(20)	$d[\text{cA93}]/dt = J_{6b} - J_{6bf}$
(21)	$d[\text{IAP3}]/dt = J_7$
(22)	$d[\text{c8a}]/dt = J_{p8} - J_8 + J_{8f}$
(23)	$d[\text{Bid}]/dt = -J_8 - J_{8p} + j_{\text{bidp}}$
(24)	$d[\text{c8B}]/dt = J_8 - J_{8f}$
(25)	$d[\text{tBid}]/dt = J_{8f} + J_{8fp} - j_{11} + j_{12b} - \mu \times \text{tBid} + \text{tbid0}$
(26)	$d[\text{c3B}]/dt = J_{8p} - J_{8fp}$
(27)	$d[\text{Bcl2}]/dt = -J_9 + j_{\text{bcl2p}} - j_{13}$
(28)	$d[\text{c3L}]/dt = J_9 - J_{9f}$
(29)	$d[\text{tBid}_{\text{mito}}]/dt = j_{11} - j_{12a} - \mu \times \text{tBid}_{\text{mito}}$
(30)	$d[\text{tBidBax}]/dt = j_{12a} - j_{12b} - \mu \times \text{tBidBax}$
(31)	$d[\text{Bax}]/dt = j_{\text{bax}} - j_{12a} - j_{12b} - j_{13}$
(32)	$d[\text{Bax2}]/dt = j_{12b} - \mu \times \text{Bax2}$
(33)	$d[\text{Cc}_{\text{mito}}]/dt = j_{\text{Ccmito}} - j_{14} - \text{MPTP} \times \text{Cc}_{\text{mito}}$

Table 4.15. Mathematical expression of model 2 in terms of ordinary differential equations

Equation Index	Ordinary Differential Equations of Model 2
(1)	$d[\text{NO}]/dt = r_{1\text{NO}} - r_{4\text{NO}} - 2r_{12\text{aNO}} - r_{12\text{bpNO}} + r_{12\text{bmNO}} + 2r_{14\text{NO}} - r_{15\text{NO}} - r_{16\text{NO}}$
(2)	$d[\text{O}_2^-]/dt = r_{2\text{NO}} - r_{4\text{NO}} - r_{5\text{NO}} - r_{10\text{NO}} - 2r_{17\text{Bno}}$
(3)	$d[\text{ONOO}^-]/dt = r_{4\text{NO}} - r_{6\text{NO}} - r_{7\text{NO}} - r_{8\text{NO}} - r_{9\text{NO}}$
(4)	$d[\text{GSH}]/dt = r_{3\text{NO}} - r_{6\text{NO}} - r_{11\text{NO}} + 2r_{\text{m}} - r_{17\text{NO}} - 2r_{17\text{bNO}}$
(5)	$d[\text{GSNO}]/dt = r_{6\text{NO}} - 2r_{10\text{NO}} + r_{11\text{NO}} - 2r_{14\text{NO}} + r_{17\text{NO}}$
(6)	$d[\text{N}_2\text{O}_3]/dt = -r_{11\text{NO}} + r_{12\text{bpNO}} - r_{12\text{bmNO}} - r_{13\text{NO}}$
(7)	$d[\text{NO}_2]/dt = 2r_{12\text{aNO}} - r_{12\text{bpNO}} + r_{12\text{bmNO}}$
(8)	$d[\text{CcO}_x]/dt = -r_{15\text{NO}}$
(9)	$d[\text{FeL}_n]/dt = -r_{16\text{NO}} + r_{17\text{NO}}$

Table 4.16. Mathematical expressions of additional reactions of model 3 in terms of ordinary differential equations

Equation Index	Ordinary Differential Equations of Model 3
(1)	$d[\text{ONOO}^-]/dt = r_{4\text{NO}} - r_{6\text{NO}} - r_{7\text{NO}} - r_{8\text{NO}} - r_{9\text{NO}} - r_{18\text{NO}}$
(2)	$d[\text{MPTP}_{\text{c1}}]/dt = -r_{18\text{NO}}$
(3)	$d[\text{N}_2\text{O}_3]/dt = -r_{11\text{NO}} + r_{12\text{bpNO}} - r_{12\text{bmNO}} - r_{13\text{NO}} - r_{19\text{NO}}$
(4)	$d[\text{c8a}]/dt = J_{\text{p8}} - J_8 + J_{8\text{f}} - r_{19\text{NO}} - r_{20\text{NO}}$
(5)	$d[\text{FeL}_n\text{NO}]/dt = r_{16\text{NO}} - r_{17\text{NO}} - r_{20\text{NO}} - r_{21\text{NO}} - r_{22\text{NO}}$
(6)	$d[\text{FeL}_n]/dt = -r_{16\text{NO}} + r_{17\text{NO}} + r_{20\text{NO}} + r_{21\text{NO}} + r_{22\text{NO}}$
(7)	$d[\text{c9a}]/dt = J_4 + J_{4\text{b}} - J_5 - J_6 + J_{6\text{f}} + j_{\text{p9a}} - r_{21\text{NO}}$
(8)	$d[\text{c3a}]/dt = J_{6\text{f}} + J_{6\text{bf}} - J_7 - J_8 + J_{8\text{f}} - J_9 + J_{9\text{f}} - \mu \times \text{c3a} - r_{22\text{NO}}$
(9)	$d[\text{Cc}]/dt = j_{14} - J_1 - \mu \times \text{Cc} + k[\text{MPTP}][\text{Cc}_{\text{mito}}]$ where $k = 1 \mu\text{M}^{-1}\text{s}^{-1}$

4.3.4. Analysis Using Bistable Apoptosis Models

Initiating an apoptotic process requires a necessary amount of the executioner pro-apoptotic caspase-3 protein. Therefore, whether a cell will die or survive is dependent on the concentration of caspase-3. In this study, it is assumed that if the caspase-3 concentration is above a threshold value of 1 nM (1×10^{-9} M), then apoptosis, and if it is below this value, then cell survival will occur. This threshold value is reached upon by a simple calculation to obtain 2500 caspase-3 molecules, which is thought to be sufficient for the onset of apoptosis. This calculation is given in Appendix B.

4.4. Simulations of The Models

4.4.1. Simulations Using Existing Models

A bistable mitochondria-dependent apoptosis model developed by Bagci *et al.* (2006) assumes cooperativity in apoptosome formation. As mentioned in section 4.1, their apoptosis model without considering NO effects is referred to as model 1 in this thesis. For different initial pro-apoptotic protein concentrations, model 1 gives both apoptotic and cell survival states in the presence of cooperativity ($p=4$). When the initial concentration of pro-apoptotic caspase-8 is high ($1 \mu\text{M}$), then the apoptotic state is obtained. As shown in Figure 4.22 obtained from XPPAUT, the steady state concentration of caspase-3 is above $5 \times 10^{-3} \mu\text{M}$ (5.15 nM), which is above the threshold concentration for the onset of apoptosis (1 nM). On the other hand, when the initial concentration of pro-apoptotic caspase-8 is low ($1 \times 10^{-5} \mu\text{M}$), then the steady state concentration of caspase-3 becomes very close to 0 as shown in Figure 4.23, so that cell survival state is reached in the case of presence of cooperativity ($p=4$).

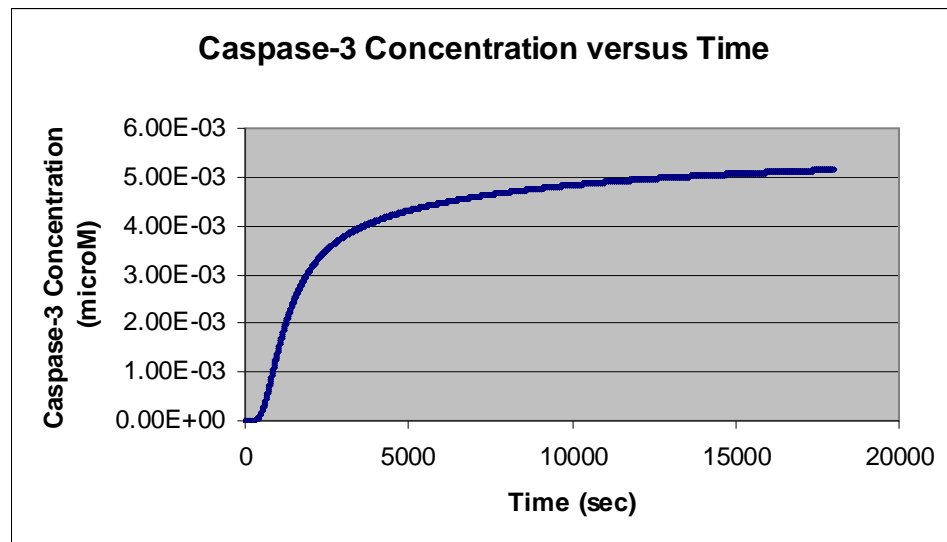


Figure 4.22. Apoptotic state of model 1 by Bagci *et al.* (2008) in the presence of cooperativity in apoptosome formation ($p=4$)

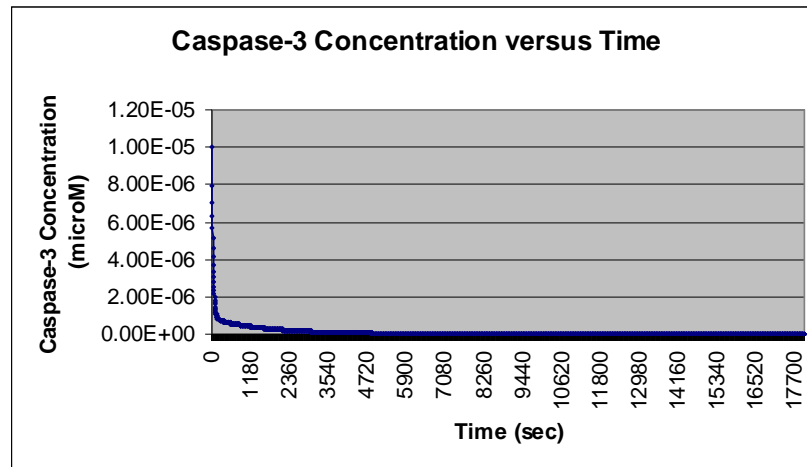


Figure 4.23. Cell survival state of model 1 by Bagci *et al.* (2008) in the presence of cooperativity in apoptosome formation ($p=4$)

In Figure 4.24, NO effects on the apoptotic pathway is considered (model 3) and it is observed that caspase-3 concentration exceeds the threshold value for the onset of apoptosis (reaches to $4.30 \times 10^{-3} \mu\text{M} = 4.30 \text{ nM}$), and then sharply falls to zero. This sharp fall is due to inhibitory effect of FeL_nNO on both caspase-3 and caspase-9. However, apoptosis will take place as caspase-3 concentration stays above the threshold value for times well above 600 seconds (which is believed to be the duration of apoptosis). In model 3, bistability is lost in the presence of NO species reactions and indistinguishable responses are obtained whether high or low pro-apoptotic protein initial concentrations are used in the presence of cooperativity ($p=4$) in apoptosome formation.

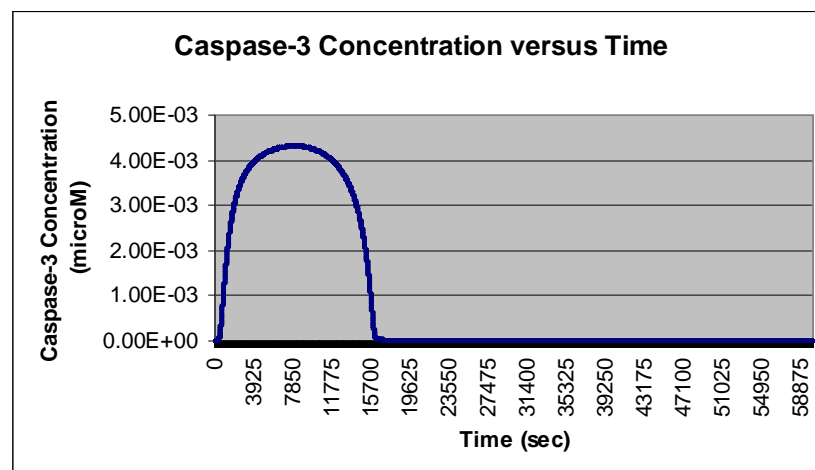


Figure 4.24. Apoptotic state of model 3 (including NO effects) by Bagci *et al.* (2008) in the presence of cooperativity in apoptosome formation ($p=4$)

The simulations for model 3 of Bagci *et al.* (2008) are repeated in the case of lack of cooperativity in apoptosome formation. The time variation of caspase-3 concentration when there is no cooperativity ($p=1$) is given in Figure 4.25 and is very similar to the case when there is cooperativity ($p=4$) except that caspase-3 concentration now reaches to a slightly higher value of 5.4 nM which is again an apoptotic state.

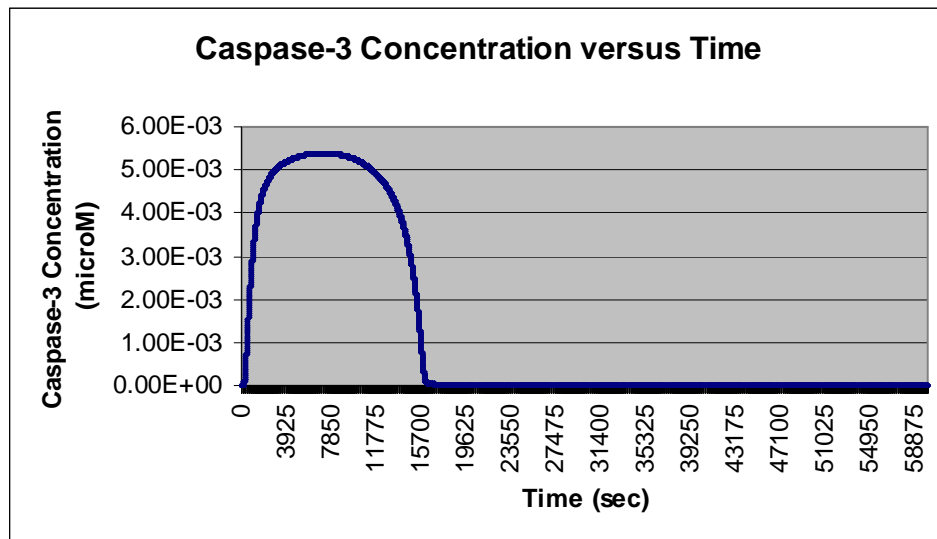


Figure 4.25. Apoptotic state of model 3 (including NO effects) by Bagci *et al.* (2008) in the lack of cooperativity in apoptosome formation ($p=1$)

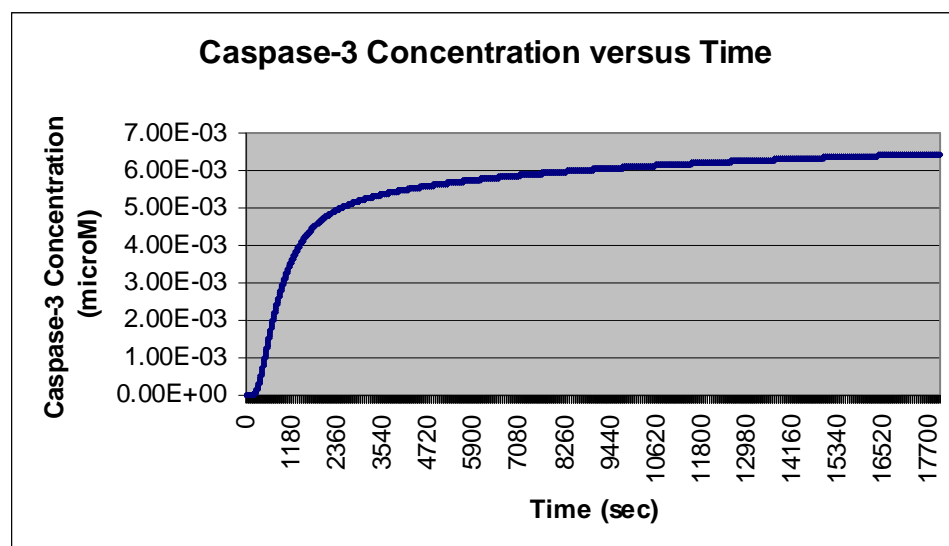


Figure 4.26. Apoptotic state of model 1 by Bagci *et al.* (2008) in the lack of cooperativity in apoptosome formation ($p=1$)

In the case of lack of cooperativity in apoptosome ($p=1$), the cell survival state is lost for model 1 and only apoptotic state ($[\text{caspase-3}]=6.44 \text{ nM}$) is obtained which does not depend on the initial concentration of pro-apoptotic caspase-8 protein as shown in Figure 4.26. Therefore, cooperativity in apoptosome formation is a necessary condition for bistable character of apoptosis according to Bagci *et al.* (2008). However, there is a controversy about the presence of cooperativity in the formation of apoptosome. Because of this, in this study the alternative apoptosis model having bistable character even in the lack of cooperativity in apoptosome is developed.

4.4.2. Analysis on Model 1 (Without NO Effects)

Firstly, analysis on the bistable model 1 (model without NO effects) is carried out for different initial conditions in the cell. When the initial concentration of HSP70, hence inhibition of apoptosome formation is high ($3.15 \text{ }\mu\text{M}$), steady state concentration of executioner caspase-3 protein reaches to an apoptotic value (higher than 1 nM) of $4.77 \times 10^{-3} \text{ }\mu\text{M}$ (4.77 nM) as shown in the Figure 4.27.

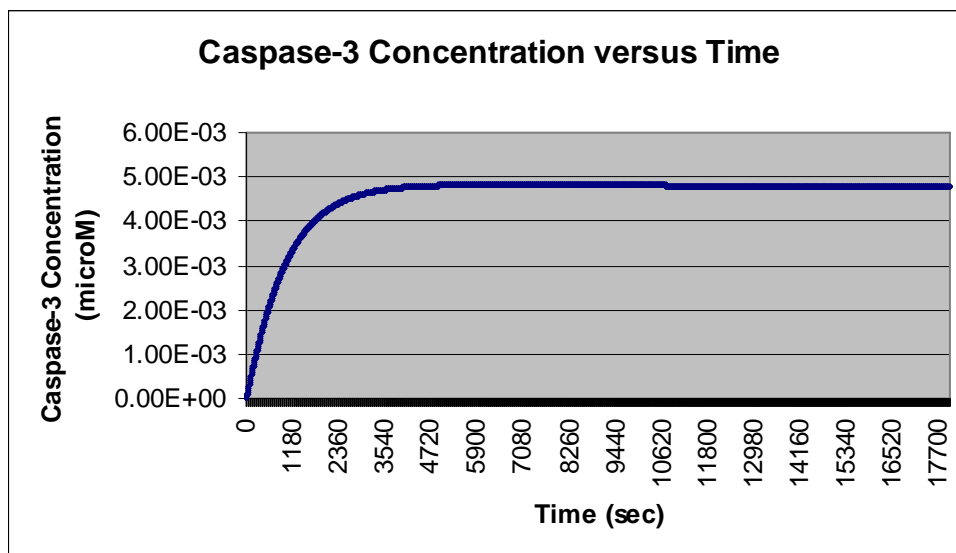


Figure 4.27. Caspase-3 concentration profile in model 1 ($[\text{HSP70}]_0 = 3.15$)

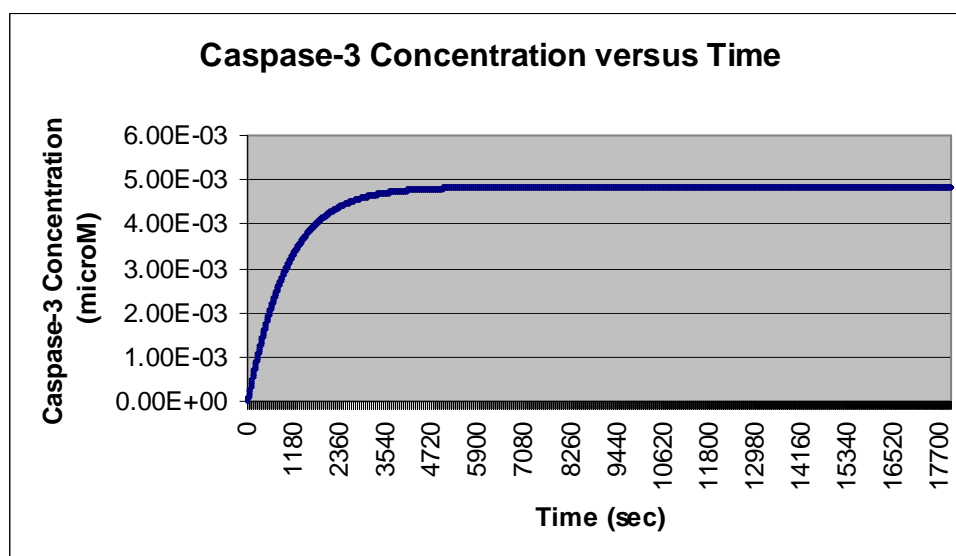


Figure 4.28. Caspase-3 concentration profile in model 1 ($[\text{HSP70}]_0 = 0.15$)

Depending on the initial value of HSP70 inhibitory protein, components of the model 1 can achieve another apoptotic state, as shown in Figure 4.28. When the initial concentration of HSP70 is low ($0.15 \mu\text{M}$), the steady state concentration of executioner caspase-3 protein becomes 4.81 nM . It can be concluded that the inhibition effect of HSP70 on apoptosis is negligible. Though very close to each other, there are two stable states both of which are apoptotic. To move one of these apoptotic states to cell survival state, NO species reactions are taken into account which constituted model 2.

4.4.3. NO Species Formation Model (Model 2)

Nitric oxide is a reactive compound and very critical for the apoptotic pathway, because it has both pro- and anti-apoptotic effects on the apoptosis. Model 2 contains the NO reactions causing formation of NO species which have important role on apoptosis. Interplays of NO species with glutathione (GSH) also reduce the oxidative stress in the cell as mentioned in section 4.2. The simulations show that bistable model 2 reaches two separate states depending on the initial conditions of GSH and NO. When the initial concentration of NO is high and GSH is low, the integration of the coupled ODEs gives rise to stable state. The steady state values of components of model 2 are given in Figure

4.29. It can be seen from this figure that the anti-apoptotic N_2O_3 and FeL_nNO (FELNOSTF in Figures 4.29 and 4.30) concentrations are negligible in the steady state.

Time	N_2O_3	GSH	NO	O ₂ H	ONOOH
60000	3.160218e-13	356.4717	0.02489158	7.069138	39.18975
Time	GSNO	NO ₂	CCOX	FEL	FELNOSTF
60000	108.5741	1.206427e-09	0	0.04999994	6.400858e-08

Figure 4.29. Stable steady state solution of model 2

Time	N_2O_3	GSH	NO	O ₂ H	ONOOH
60000	3345.528	0.0008195021	3883.798	0.0001619773	4.911043e+07
Time	GSNO	NO ₂	CCOX	FEL	FELNOSTF
60000	485.4197	63.43087	0	5.754625e-07	0.049999942

Figure 4.30. Unstable state of model 2

In the case of low initial concentration of NO and high initial concentration of GSH, the integration of the model equations gives rise to an unstable state. Note that one of the two states is also given as being unstable by CRNT. In this state, concentration run-aways of NO species ($ONOO^-$, FeL_nNO , N_2O_3) are observed and their concentrations are reached to very high values as shown in Figure 4.30. This is not a plausible situation in the cell condition and extreme concentrations of some oxidizing species such as NO and $ONOO^-$ may cause cell death not due to apoptosis, but necrosis.

4.4.4. Analysis on Combined Model (Model 3)

Two bistable models, model 1 and model 2, are combined to form model 3 in order to include NO effects into model 1. This model 3 is then used for investigating the apoptotic pathway with NO effects for different initial conditions. The combination of model 1 (has two stable states) and model 2 (has one stable and one unstable state) gives rise to four steady states which are;

- Model 311 (combination of steady state I of model 1 and unstable state of model 2),
- Model 312 (combination of steady state I of model 1 and stable state of model 2),
- Model 321 (combination of steady state II of model 1 and unstable state of model 2),
- Model 322 (combination of steady state II of model 1 and stable state of model 2).

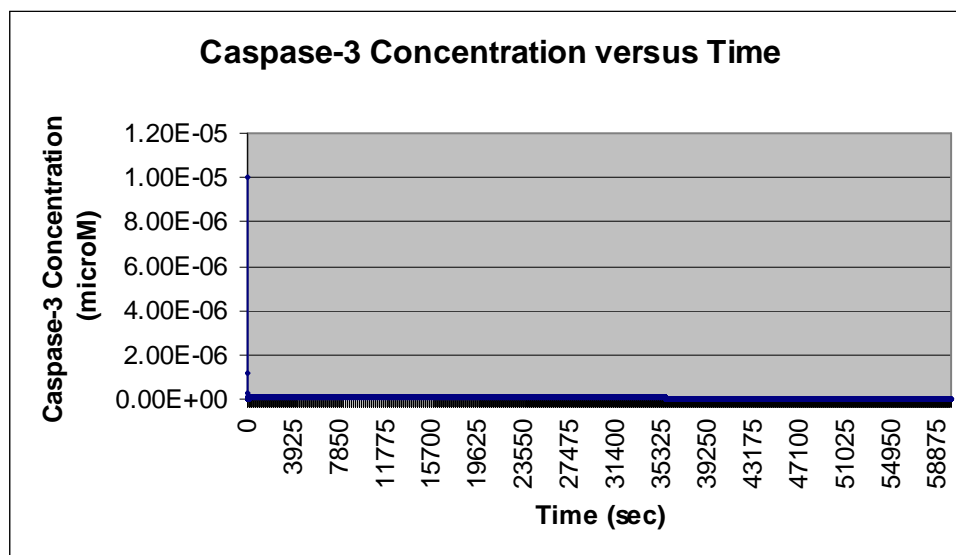


Figure 4.31. Caspase-3 concentration profile in the cell survival state I (simulation of model 311)

Model 311, for the initial concentrations given, combines the lower apoptotic state (steady state caspase-3 concentration equals to 4.77 nM) of model 1 with that of the model 2 which gives very high concentrations of NO species. The simulation of this model shows that cell survival state exists as shown in Figure 4.31, since the concentration of caspase-3 converges to $3.89 \times 10^{-8} \mu\text{M}$ (or equivalently $3.89 \times 10^{-5} \text{ nM}$). This value is well below the necessary amount of caspase-3 for the onset of apoptosis. In Table 4.17, it can be seen that steady state concentration of pro-apoptotic caspase-8 protein goes to zero. Moreover, NO species (N_2O_3 , ONOO^- and FeL_nNO) converge to high steady state values of 1182.64, 1.76×10^7 and $0.04999 \mu\text{M}$ respectively. It should be noted that maximum concentration of FeL_nNO that it can raise, is restricted with the initial concentration of FeL_n , which is $0.05 \mu\text{M}$. The existence of cell survival state can be explained by the dominant effect of anti-apoptotic proteins N_2O_3 and FeL_nNO over the effect of ONOO^- and the high initial concentration of caspase-8.

Table 4.17. Steady state concentrations of critical species in simulation of model 311

Species	Steady State Concentration (μM)
Caspase-8	0
Cytochrome <i>c</i>	0.00173
Apoptosome	0.01255
Apop.(Caspase-9) ₂	2.65×10^{-5}
Caspase-9	0.0001
Caspase-3	3.89×10^{-8}
NO	2064.96
GSH	0.0023
N ₂ O ₃	1182.64
ONOO ⁻	1.76×10^7
FeL _n NO	0.04999

Model 312 combines the lower apoptotic state of model 1 and the stable state of model 2 in which, among the steady state concentrations of NO species, N₂O₃ and FeL_nNO converge practically zero and pro-apoptotic ONOO⁻ is non-zero. The simulation of this model results in the existence of apoptotic steady state as given in Figure 4.32. Steady state concentration of caspase-3 is 0.0085 μM (=8.5 nM), which is well above the threshold value for the onset of apoptosis. In this state, it can be observed from Table 4.18 that the apoptosome formation and the protein concentrations (Apop.(Caspase-9)₂ and Caspase-9) for the activation of executioner caspase-3 are higher in comparison with simulation of model 311 which gives cell survival state. Moreover, it can also be seen that anti-apoptotic NO species (N₂O₃ and FeL_nNO) concentrations are low in this case, consequently cell survival state cannot be reached and the apoptotic state dominates. At this state, caspase-3 concentration is higher in comparison with the steady state of model 1 (4.77 nM), which is the effect of high pro-apoptotic ONOO⁻ concentration (141.05 μM).

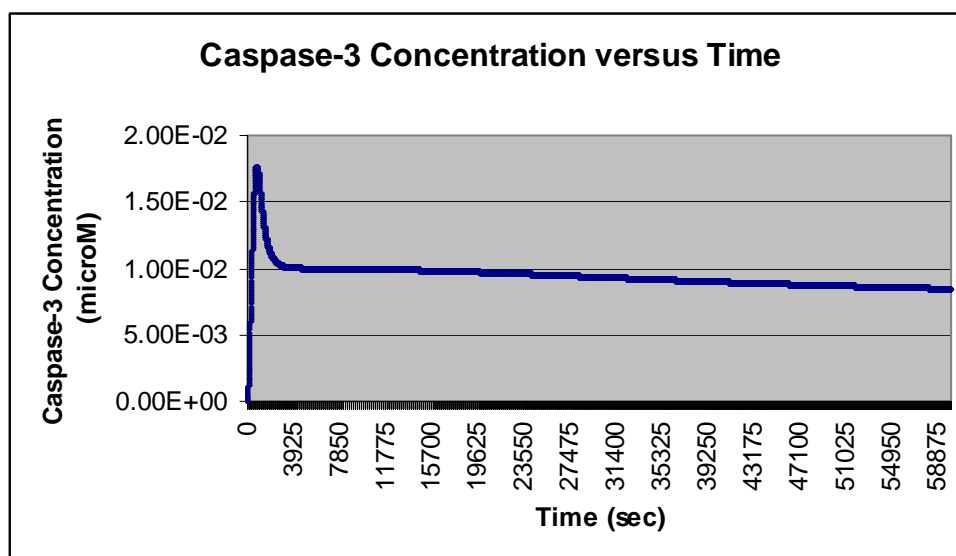


Figure 4.32. Caspase-3 concentration profile in the apoptotic state I (simulation of model 312)

Table 4.18. Steady state concentrations of critical species in simulation of model 312

Species	Steady State Concentration (μM)
Caspase-8	0
Cytochrome <i>c</i>	0.0044
Apoptosome	0.0182
Apop.(Caspase-9) ₂	2.95×10^{-5}
Caspase-9	0.0612
Caspase-3	0.0085
NO	0.0310
GSH	184.43
N ₂ O ₃	3.31×10^{-12}
ONOO ⁻	141.05
FeL _n NO	6×10^{-6}

Model 321 combines the higher apoptotic state of model 1 (steady state concentration of caspase-3 is 4.81 nM) and unsteady state of model 2. Simulation of this model 321 another cells survival state appears because of insufficient production of caspase-3 ($6.11 \times 10^{-8} \mu\text{M}$) as shown in Figure 4.33. In Table 4.19, it can again be observed that anti-apoptotic NO species concentration are high. Although, the pro-apoptotic ONOO⁻ reaches to high steady state values, the dominance of FeL_nNO and N₂O₃ causes the inhibition of caspase-9 and caspase-3 and hence the existence of cell survival state.

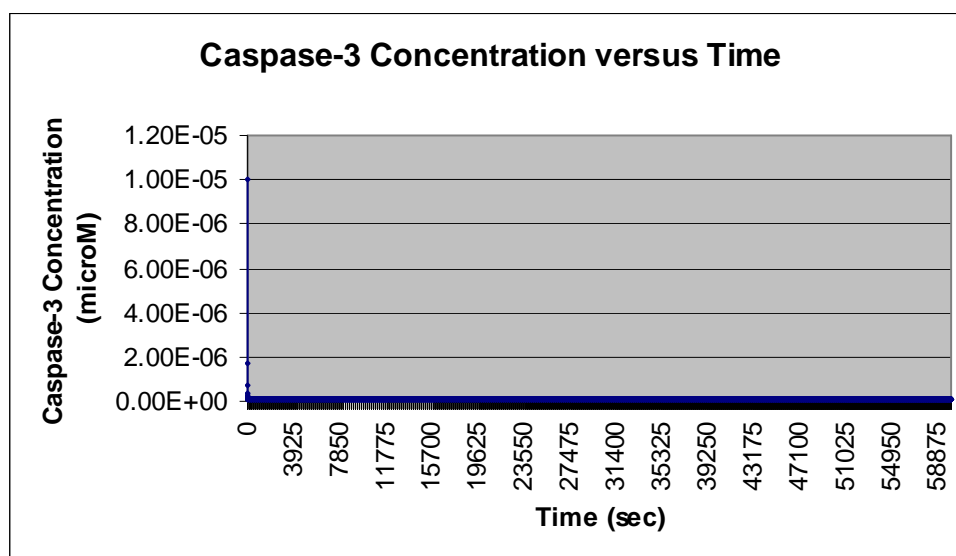


Figure 4.33. Caspase-3 concentration profile in the cell survival state II (simulation of model 321)

Table 4.19. Steady state concentrations of critical species in simulation of model 321

Species	Steady State Concentration (μM)
Caspase-8	0
Cytochrome <i>c</i>	0.00197
Apoptosome	5.755
Apop.(Caspase-9) ₂	4.16×10^{-5}
Caspase-9	0.00016
Caspase-3	6.11×10^{-8}
NO	2064.95
GSH	0.0026
N ₂ O ₃	1043.17
ONOO ⁻	1.55×10^7
FeL _n NO	0.04999

Finally, the results of the last simulation, simulation of model 322, which combines higher apoptotic state of model 1 and stable steady state of model 2, show that another apoptotic state exists for the given initial conditions within the cell as shown in Figure 4.34. Table 4.20 shows that steady state concentration of caspase-3 in this new apoptotic state is higher than the first apoptotic state and converges to 0.0112 μM or equivalently 11.2 nM. The existence of the apoptotic state is due to low production rate of anti-apoptotic NO species, and sufficiently higher production rate of pro-apoptotic caspases and complexes.

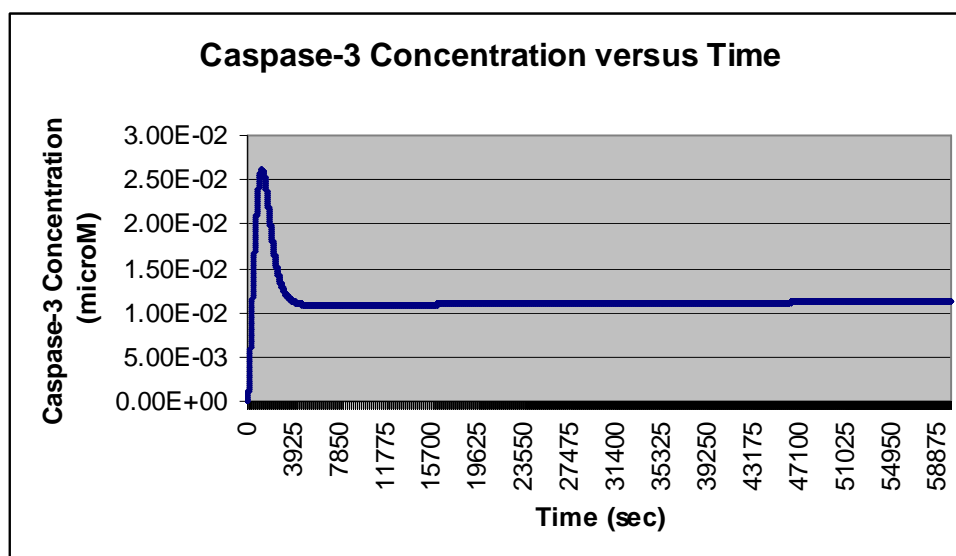


Figure 4.34. Caspase-3 concentration profile in the apoptotic state II (simulation of model 322)

Table 4.20. Steady state concentrations of critical species in simulation of model 322

Species	Steady State Concentration (μM)
Caspase-8	0
Cytochrome <i>c</i>	0.00471
Apoptosome	5.81
Apop.(Caspase-9) ₂	0.000548
Caspase-9	0.0879
Caspase-3	0.01123
NO	0.0310
GSH	184.43
N ₂ O ₃	3.31×10^{-12}
ONOO ⁻	141.05
FeL _n NO	6×10^{-6}

In summary, the existence of cell survival states can be explained by the dominant effect of anti-apoptotic NO species (FeL_nNO and N₂O₃) over pro-apoptotic ONOO⁻, which cause inhibition of caspases and complexes which are indispensable for apoptosis. The dominance of the anti-apoptotic proteins over the pro-apoptotic ONOO⁻ can be possibly explained in two ways. One reason is that the reaction rate constant of the interaction of ONOO⁻ with the pro-apoptotic protein Mitochondria Permeability Transition Pores (MPTPs) has the lowest reaction rate value compared to other NO species with other pro-apoptotic proteins such as caspase-3 and caspase-9. The second reason is that ONOO⁻

behaves pro-apoptotically by increasing the number of MPTPs. These pores play a crucial role for the transfer of the cytochrome *c* (cyt *c*) from mitochondria to the cytosol. Increasing cyt *c* in cytosol in turn increases the number of the Apaf-1/cyt *c* complex which is responsible for the formation of apoptosome. This enhances the apoptosis by promoting the cleavage of procaspase-3. Therefore, if the number of cyt *c* in the mitochondria is low, while the concentration of ONOO⁻ is high; this will not be effective for the apoptosis to occur. Hence, anti-apoptotic effect of the NO species will be more dominant and the monostable cell survival state will be observed. Consequently, their anti-apoptotic effect is crucial for the bistable character of the apoptotic pathway, when there is no cooperativity in apoptosome formation. It should also be noted that steady state concentrations in apoptotic states of model 3 are higher than those of model 1. This situation can be explained by the pro-apoptotic effect of ONOO⁻, since concentrations of anti-apoptotic N₂O₃ and FeL_nNO are very close to zero in the apoptotic state.

5. CONCLUSIONS AND RECOMMENDATIONS

5.1. Conclusions

In a previous study, Bagci *et al.* (2006) expressed the sequence of chemical reactions and physical interactions in the apoptotic pathway in terms of coupled ordinary differential equations and inferred the bistability of the model from the steady state values of caspase-3 concentrations. For instance, when the initial concentration of a pro-apoptotic protein such as caspase-8 is low, caspase-3 concentration converges to zero i.e. cell survival occurs. On the other hand, if the initial concentration of a pro-apoptotic protein such as caspase-8 is high, caspase-3 concentration attains a constant value that is sufficient (5.15 nM) for the onset of apoptosis (higher than 1 nM). In this model, the cooperativity constant p of Apaf-1/cyt c forming apoptosome was taken as 4. Moreover, it was observed that the bistable behavior of the model is lost when the cooperativity constant is taken as 1. In this case, the concentration of caspase-3 converges to apoptotic value 6.44 nM which is greater than the threshold value of caspase-3 concentration needed for the onset of apoptosis and monostable apoptosis state exists.

Cooperativity in apoptosome formation is a controversial issue and therefore in this study, the cooperativity constant, p , is taken as 1 by assuming that the formation of apoptosome lacks cooperativity. It is also expected that the bistable behavior of the model can be observed by the addition of inhibitors such as inhibitory heat shock protein HSP70 as an inhibitor of the apoptosome formation. This indeed resulted in bistability. In order to determine the multistability (in this case bistability) of the apoptotic pathway expressed as a series of reactions is checked using Chemical Reaction Network Toolbox developed by Feinberg. Since, CRNT toolbox is limited to 20 complexes a modular approach is adapted for determining multistability capacity of the reaction network. The whole model is divided into small modules, then whether multiplicity exists in each module is checked independently. This hinges upon the assumption that bistable character in a module inside the model is preserved. Therefore, the multistability analysis is carried out for different

modules inside the model. These modules are created in a way that they include circularity and causality. It is not guaranteed that a model has multistable character if it includes circulatory and causality, but these features are good indicators of bistability for most cases. Also, it is believed that the circularity inside a model is a necessary condition for the multistable behavior of the module because of causing or increasing the nonlinearity of the coupled ordinary equations (Saez-Rodriguez *et al.*, 2008). Consequently, lowering the number of equations in a model using this modularity concept helped to determine the multistability successfully in the whole model.

It is found out that formation of caspase-9 with the interaction of apoptosome and procaspase-9 (cleavage of procaspase-9 and activation of caspase-9) in the presence of HSP70 inhibitor has capacity for multiequilibria both of which are apoptotic. This situation can be explained by the inhibitory effect that causes to achieve lower concentration of caspase-3. However, in the absence of HSP70 the module converges to monostable apoptotic state. This model through predicting bistability is not desired since both states are apoptotic. On the other hand, the bistability that is expected for a healthy individual is to have one stable cell survival state and one stable apoptotic state which is not provided by this model. Hence, this model is further expanded to include NO species effects.

The apoptotic pathway involving NO effects (model 2) is separated into three modules (compartments). Basically, these modules are ONOO⁻ module, N₂O₃ module, and FeL_nNO module. Among these modules, it is found out that ONOO⁻ module does have the capacity for multistability, one being stable and the other is unstable. However, other modules (N₂O₃ module and FeL_nNO module) cannot admit steady states with positive concentrations. Therefore, the overall module is built around this ONOO⁻ module along with caspase-9 activation module. To this end, kinetic parameters as obtained from CRNT for the bistable module are combined with the kinetic parameters of the other modules, which are taken from the literature. After the completion of the whole model, the analysis is carried out on model 3. Depending on the initial cell conditions, four steady states are obtained by integrating the coupled ODEs of the apoptosis model using XPPAUT. Two of these states are apoptotic states in which steady state concentrations of caspase-3 are

higher than the threshold value for the onset of apoptosis, (8.5 nM and 11.2 nM). The remaining two states are cell survival states, in which steady state concentration of caspase-3 is very close to zero. In conclusion, the anti-apoptotic effects of NO are crucial to obtain bistability, namely cell survival and apoptotic states in a cell.

5.2. Recommendations

The modeling of apoptotic pathway is a very widely studied topic, since the understanding of this pathway is critical for the cancer and neurological diseases treatments. The main development that can be made on the model could be the expansion of the model by the addition of components proposed from recent studies with their experimentally obtained kinetic parameters. Moreover, reactions in other pathways such as cell cycle, in which pro-apoptotic proteins e.g. p53 is involved, can be added into the pathway so as to include interaction effects of different pathways. This way a more comprehensive model can be developed. However, determination of kinetic constants will constitute a problem, since providing accurate biological parameters is very difficult.

In the unstable state of model 2, the ONOO^- concentration increases without any bound. This is because NO is produced at a concentrate without any inhibition. This problem can be resolved, for example, including an inhibition effect of ONOO^- to the production rate of NO either directly or indirectly.

The model used in this thesis is for a general tissue cell, which can be extended to specific cells such as hepatocytes and lymphocytes. This can be done by the knowledge of average cell conditions for these cell types. Moreover, if clinical tests can be used determine a patient's cell conditions from microarray data, then computer simulation can be carried out to find out an optimum treatment strategy.

APPENDIX A: REACTION EXPRESSIONS AND PARAMETERS USED IN THE SIMULATION

A.1. Model 1

Table A.1. Reactions of the mitochondria-dependent apoptosis model (model 1)

Index	Reactions of Model I	Forward Reaction Rate Expressions	Forward Reaction Rate Expressions
(1)	$Cc + Ap \leftrightarrow Cc.Ap$	$r_{1p}=k_{1p}[Cc][Ap]$	$r_{1m}=k_{1m}[CcAp]$
(1b)	$7 CcAp \leftrightarrow Apop$	$r_{1bp}=k_{1bp}[CcAp]^p$	$r_{1bm}=k_{1bm}[Apop]$
(2)	$Apop + c9z \leftrightarrow Apopc9z$	$r_{2p}=k_{2p}[Apop][c9z]$	$r_{2m}=k_{2m}[Apopc9z]$
(3)	$Apopc9z + c9z \leftrightarrow Apopc9z2$	$r_{3p}=k_{3p}[Apopc9z][c9z]$	$r_{3m}=k_{3m}[Apopc9z2]$
(3f)	$Apopc9z2 \Rightarrow Apopc9a2$	$r_{3f}=k_{3f}[Apopc9z2]$	
(4)	$Apopc9a2 \leftrightarrow Apopc9a + c9a$	$r_{4p}=k_{4p}[Apopc9a2]$	$r_{4m}=k_{4m}[Apopc9a][c9a]$
(4b)	$Apopc9a \leftrightarrow Apop + c9a$	$r_{4bp}=k_{4bp}[Apopc9a]$	$r_{4bm}=k_{4bm}[Apop][c9a]$
(15)	$Apop + HSP70 \leftrightarrow ApopHSP$	$r_{15p}=k_{15p}[Apop][HSP70]$	$r_{15m}=k_{15m}[ApopHSP]$
(5)	$c9a + IAP \leftrightarrow IAP9$	$r_{5p}=k_{5p}[c9a][IAP]$	$r_{5m}=k_{5m}[IAP9]$
(5b)	$Apopc9a + IAP \leftrightarrow IAPA9$	$r_{5bp}=k_{5bp}[Apopc9a][IAP]$	$r_{5bm}=k_{5bm}[IAPA9]$
(5c)	$Apopc9a2 + IAP \leftrightarrow IAPA29$	$r_{5cp}=k_{5cp}[Apopc9a2][IAP]$	$r_{5cm}=k_{5cm}[IAPA29]$
(6)	$c3z + c9a \leftrightarrow c93$	$r_{6p}=k_{6p}[c3z][c9a]$	$r_{6m}=k_{6m}[c93]$
(6f)	$c93 \Rightarrow c3a + c9a$	$r_{6f}=k_{6f}[c93]$	
(6b)	$c3z + Apopc9a2 \leftrightarrow cA93$	$r_{6bp}=k_{6p}[c3z][Apopc9a2]$	$r_{6bm}=k_{6m}[cA93]$
(6bf)	$cA93 \Rightarrow c3a + Apopc9a2$	$r_{6bf}=k_{6f}[cA93]$	
(7)	$c3a + IAP \leftrightarrow IAP3$	$r_{7p}=k_{7p}[c3a][IAP]$	$r_{7m}=k_{7m}[IAP3]$
(8)	$c8a + Bid \leftrightarrow c8B$	$r_{8p}=k_{8p}[c8a][Bid]$	$r_{8m}=k_{8m}[c8B]$
(8f)	$c8B \Rightarrow c8a + tBid$	$r_{8f}=k_{8f}[c8B]$	
(8)	$c3a + Bid \leftrightarrow c3B$	$r_{8pp}=k_{8p}[c3a][Bid]$	$r_{8mp}=k_{8m}[c3B]$
(8f)	$c3B \Rightarrow c3a + tBid$	$r_{8fp}=k_{8f}[c3B]$	
(9)	$c3a + Bcl2 \leftrightarrow c3L$	$r_{9p}=k_{9p}[c3a][Bcl2]$	$r_{9m}=k_{9m}[c3L]$
(9f)	$c3L \Rightarrow c3a + B2c$	$r_{9f}=k_{9f}[c3L]$	
(11)	$tBid \Rightarrow tBid_{mito}$	$r_{11}=k_{11}[tBid]$	
(12a)	$tBid_{mito} + Bax \Rightarrow tBidBax$	$r_{12a}=k_{12a}[tBid_{mito}][Bax]$	
(12b)	$tBidBax + Bax \Rightarrow tBid + Bax2$	$r_{12b}=k_{12b}[tBidBax][Bax]$	
(13)	$Bcl2 + Bax \Rightarrow 0$	$r_{13}=k_{13}[Bcl2][Bax]$	
(14)	$Bax2 + Cc_{mito} \Rightarrow Cc + Bax2$	$r_{14}=k_{14}[Bax2][Cc_{mito}]$	

Table A.2. Reaction rate constants of the mitochondria-dependent apoptosis model (model 1)

Index	Reaction of Model I	Forward Reaction Rate Constants	Backward Reaction Rate Constants
(1)	$Cc + Ap \Leftrightarrow Cc.Ap$	$k_{1p} = 5 \mu M^{-1} s^{-1}$	$k_{1m} = 0.5 s^{-1}$
(1b)	$7 CcAp \Leftrightarrow Apop$	$k_{1bp} = 50,000 s^{-1}$	$k_{1bm} = 0.5 s^{-1}$
(2)	$Apop + c9z \Leftrightarrow Apopc9z$	$k_{2p} = 10.23 \mu M^{-1} s^{-1}$	$k_{2m} = 3.19 s^{-1}$
(3)	$Apopc9z + c9z \Leftrightarrow Apopc9z2$	$k_{3p} = 5.14 \mu M^{-1} s^{-1}$	$k_{3m} = 1 s^{-1}$
(3f)	$Apopc9z2 \Rightarrow Apopc9a2$	$k_{3f} = 2.72 s^{-1}$	
(4)	$Apopc9a2 \Leftrightarrow Apopc9a + c9a$	$k_{4p} = 6.39 s^{-1}$	$k_{4m} = 0.59 \mu M^{-1} s^{-1}$
(4b)	$Apopc9a \Leftrightarrow Apop + c9a$	$k_{4bp} = 13.05 s^{-1}$	$k_{4bm} = 1.60 \mu M^{-1} s^{-1}$
(15)	$Apop + HSP70 \Leftrightarrow ApopHSP$	$k_{15p} = 4.03 \mu M^{-1} s^{-1}$	$k_{15m} = 1 s^{-1}$
(5)	$c9a + IAP \Leftrightarrow IAP9$	$k_{5p} = 5 \mu M^{-1} s^{-1}$	$k_{5m} = 0.0035 s^{-1}$
(5b)	$Apopc9a + IAP \Leftrightarrow IAPA9$	$k_{5bp} = 5 \mu M^{-1} s^{-1}$	$k_{5bm} = 0.0035 s^{-1}$
(5c)	$Apopc9a2 + IAP \Leftrightarrow IAPA29$	$k_{5cp} = 5 \mu M^{-1} s^{-1}$	$k_{5cm} = 0.0035 s^{-1}$
(6)	$c3z + c9a \Leftrightarrow c93$	$k_{6p} = 10 \mu M^{-1} s^{-1}$	$k_{6m} = 0.5 s^{-1}$
(6f)	$c93 \Rightarrow c3a + c9a$	$k_{6f} = 0.001 s^{-1}$	
(6b)	$c3z + Apopc9a2 \Leftrightarrow cA93$	$k_{6bp} = 10 \mu M^{-1} s^{-1}$	$k_{6bm} = 0.5 s^{-1}$
(6bf)	$cA93 \Rightarrow c3a + Apopc9a2$	$k_{6bf} = 0.1 s^{-1}$	
(7)	$c3a + IAP \Leftrightarrow IAP3$	$k_{7p} = 5 \mu M^{-1} s^{-1}$	$k_{7m} = 0.0035 s^{-1}$
(8)	$c8a + Bid \Leftrightarrow c8B$	$k_{8p} = 10 \mu M^{-1} s^{-1}$	$k_{8m} = 0.5 s^{-1}$
(8f)	$c8B \Rightarrow c8a + tBid$	$k_{8f} = 0.1 s^{-1}$	
(8)	$c3a + Bid \Leftrightarrow c3B$	$k_{8p} = 10 \mu M^{-1} s^{-1}$	$k_{8m} = 0.5 s^{-1}$
(8f)	$c3B \Rightarrow c3a + tBid$	$k_{8f} = 0.1 s^{-1}$	
(9)	$c3a + Bcl2 \Leftrightarrow c3L$	$k_{9p} = 10 \mu M^{-1} s^{-1}$	$k_{9m} = 0.5 s^{-1}$
(9f)	$c3L \Rightarrow c3a + B2c$	$k_{9f} = 0.1 s^{-1}$	
(11)	$tBid \Rightarrow tBid_{mito}$	$k_{11} = 10 s^{-1}$	
(12a)	$tBid_{mito} + Bax \Rightarrow tBidBax$	$k_{12a} = 10 \mu M^{-1} s^{-1}$	
(12b)	$tBidBax + Bax \Rightarrow tBid + Bax2$	$k_{12b} = 10 \mu M^{-1} s^{-1}$	
(13)	$Bcl2 + Bax \Rightarrow 0$	$k_{13} = 10 \mu M^{-1} s^{-1}$	
(14)	$Bax2 + Cc_{mito} \Rightarrow Cc + Bax2$	$k_{14} = 10 \mu M^{-1} s^{-1}$	

Table A.3. Net formation rate equations of model 1

Equation Index	Net Formation Rates (Model I)
(1)	$J_1 = r_{1p} - r_{1m}$
(2)	$J_{1b} = r_{1bp} - r_{1bm}$
(3)	$J_2 = r_{2p} - r_{2m}$
(4)	$J_3 = r_{3p} - r_{3m}$
(5)	$J_{3f} = r_{3f}$
(6)	$J_4 = r_{4p} - r_{4m}$
(7)	$J_{4b} = r_{4bp} - r_{4bm}$
(8)	$J_{15} = r_{15p} - r_{15m}$
(9)	$J_5 = r_{5p} - r_{5m}$
(10)	$J_{5b} = r_{5bp} - r_{5bm}$
(11)	$J_{5c} = r_{5cp} - r_{5cm}$
(12)	$J_6 = r_{6p} - r_{6m}$
(13)	$J_{6f} = r_{6f}$
(14)	$J_{6b} = r_{6bp} - r_{6bm}$
(15)	$J_{6bf} = r_{6bf}$
(16)	$J_7 = r_{7p} - r_{7m}$
(17)	$J_8 = r_{8p} - r_{8m}$
(18)	$J_{8f} = r_{8f}$
(19)	$J_{8p} = r_{8pp} - r_{8mp}$
(20)	$J_{8fp} = r_{8fp}$
(21)	$J_9 = r_{9p} - r_{9m}$
(22)	$J_{9f} = r_{9f}$
(23)	$j_{11} = r_{11}$
(24)	$j_{12a} = r_{12a}$
(25)	$j_{12b} = r_{12b}$
(26)	$j_{13} = r_{13}$
(27)	$j_{14} = r_{14}$

Table A.4. Formation and degradation rate equations of model 1

(28)	$J_{Ap} = 0.0001 \times a1 - \mu \times Ap$
(29)	$J_{IAP} = 0.0001 \times a2 - \mu \times IAP$
(30)	$J_{p3} = 0.1 \times 0.0001 \times a3 - \mu \times c3z$
(31)	$J_{p8} = -\mu \times c8a$
(32)	$j_{bidp} = 0.0001 \times a5 - \mu \times Bid$
(33)	$j_{bcl2p} = 0.0001 \times a6 \times p53_{thresh}^4 / (p53^4 + p53_{thresh}^4) - \mu \times Bcl2$
(34)	$j_{bax} = 0.0001 \times a7 \times (1 + p53^4 / (p53^4 + p53_{thresh}^4)) - \mu \times Bax$
(35)	$j_{ccmito} = 0.0001 \times a8 - \mu \times Cc_{mito}$
(36)	$J_{p9} = 0.00054366$
(37)	$j_{Aph} = -0.0001 \times ApopHSP$
(38)	$j_{Hsp} = 0.0001$
(39)	$j_{p9a} = -0.0001 \times c9a$
(40)	$j_{Apop} = 0.0001$

Table A.5. Parameters used in simulation of model 1

Parameters In Model I	
(1)	$a1 = 3$
(2)	$a2 = 0.3$
(3)	$a3 = 3$
(4)	$a5 = 0.3$
(5)	$a6 = 0.8$
(6)	$a7 = 0.3$
(7)	$a8 = 3$
(8)	$a9 = 1$
(9)	$a10 = 1$
(10)	$a11 = 1$
(11)	$a12 = 1$
(12)	$a13 = 3$
(13)	$\mu = 0.002 \times a13$
(14)	$P53_{\text{thresh}} = 0.004$
(15)	cooperativity (p) = 1
(16)	$\text{nop} = 0$
(17)	$\text{tBid}_0 = 0$
(18)	$p53 = 0.0066$
(19)	$\text{MPTP} = 0$

Table A.6. Initial concentrations of components of model 1

Initial Concentrations
$[\text{CcAp}]_0 = 0 \mu\text{M}$
$[\text{Ap}]_0 = 0.004 \mu\text{M}$
$[\text{Cc}]_0 = 0 \mu\text{M}$
$[\text{IAP}]_0 = 0.004 \mu\text{M}$
$[\text{IAP9}]_0 = 0 \mu\text{M}$
$[\text{IAPA9}]_0 = 0 \mu\text{M}$
$[\text{IAPA29}]_0 = 0 \mu\text{M}$
$[\text{c9a}]_0 = 0 \mu\text{M}$
$[\text{c3z}]_0 = 0.004 \mu\text{M}$
$[\text{c3a}]_0 = 0.00001 \mu\text{M}$
$[\text{cA93}]_0 = 0 \mu\text{M}$
$[\text{IAP3}]_0 = 0 \mu\text{M}$
$[\text{Bid}]_0 = 0.004 \mu\text{M}$
$[\text{c8a}]_0 = 0.00001 \mu\text{M}$
$[\text{c8B}]_0 = 0 \mu\text{M}$
$[\text{c3B}]_0 = 0 \mu\text{M}$
$[\text{Bcl2}]_0 = 0.004 \mu\text{M}$
$[\text{c3L}]_0 = 0 \mu\text{M}$
$[\text{Bax}]_0 = 0.004 \mu\text{M}$
$[\text{Cc}_{\text{mito}}]_0 = 0.004 \mu\text{M}$

Table A.7. Initial concentrations for obtaining steady state I

$[\text{Apop}]_0 = 0.15 \mu\text{M}$
$[\text{c9z}]_0 = 2.32 \mu\text{M}$
$[\text{Apopc9z}]_0 = 0.31 \mu\text{M}$
$[\text{Apopc9z2}]_0 = 1 \mu\text{M}$
$[\text{Apopc9a2}]_0 = 0.58 \mu\text{M}$
$[\text{Apopc9a}]_0 = 0.31 \mu\text{M}$
$[\text{c9a}]_0 = 5.43 \mu\text{M}$
$[\text{HSP70}]_0 = 3.15 \mu\text{M}$
$[\text{ApopHSP}]_0 = 1 \mu\text{M}$

Table A.8. Initial concentrations for obtaining steady state II

$[\text{Apop}]_0 = 3.16 \mu\text{M}$
$[\text{c9z}]_0 = 0.31 \mu\text{M}$
$[\text{Apopc9z}]_0 = 2.32 \mu\text{M}$
$[\text{Apopc9z2}]_0 = 1 \mu\text{M}$
$[\text{Apopc9a2}]_0 = 1.59 \mu\text{M}$
$[\text{Apopc9a}]_0 = 2.33 \mu\text{M}$
$[\text{c9a}]_0 = 5.43 \mu\text{M}$
$[\text{HSP70}]_0 = 0.15 \mu\text{M}$
$[\text{ApopHSP}]_0 = 1 \mu\text{M}$

A.2. Model 2

Table A.9. NO pathway reactions effecting on apoptotic pathway (model 2)

Index	Reactions of Model 2	Reaction Rate Expressions
(1)	$0 \Rightarrow NO$	$r_{1NO} = k_{1NO}$
(2)	$0 \Rightarrow O_2^-$	$r_{2NO} = k_{2NO}$
(3)	$0 \Rightarrow GSH$	$r_{3NO} = k_{3NO}$
(4)	$NO + O_2^- \Rightarrow ONOO^-$	$r_{4NO} = k_{4NO} [NO][O_2^-]$
(5)	$SOD + O_2^- + Hp \Rightarrow SOD + 1/2 O_2 + 1/2 H_2O_2$	$r_{5NO} = k_{5NO} [SOD]^2 [O_2^-]^2$
(6)	$ONOO^- + GSH \Rightarrow GSNO + \text{products}$	$r_{6NO} = k_{6NO} [ONOO^-][GSH]$
(7)	$ONOO^- + GPX \Rightarrow GPX + \text{products}$	$r_{7NO} = k_{7NO} [ONOO^-][GPX]$
(8)	$ONOO^- + CO_2 \Rightarrow \text{products}$	$r_{8NO} = k_{8NO} [NO][CO_2]$
(9)	$ONOO^- + Cc \Rightarrow Cc + \text{products}$	$r_{9NO} = k_{9NO} [NO][\text{cyt c}]$
(10)	$2GSNO + O_2^- + H_2O \Rightarrow GSSG + \text{products}$	$r_{10NO} = k_{10NO} [GSNO]^2 [O_2^-]$
(11)	$N_2O_3 + GSH \Rightarrow GSNO + \text{products}$	$r_{11NO} = k_{11NO} [N_2O_3][GSH]$
(12a)	$2NO + O_2 \Rightarrow 2NO_2$	$r_{12aNO} = k_{12aNO} [NO]^2 [O_2]$
(13)	$N_2O_3 + H_2O \Rightarrow \text{products}$	$r_{13NO} = k_{13NO} [N_2O_3]$
(m)	$GSSG + NADPH + Hp \Rightarrow 2GSH + NADP_p$	$r_{mNO} = k_m [GSSG]$
(12bp)	$NO_2 + NO \Leftrightarrow N_2O_3$	$r_{12bpNO} = k_{12bpNO} [NO_2][NO]$
(12bm)		$r_{12bmNO} = k_{12bmNO} [N_2O_3]$
(14)	$GSNO \xrightarrow{(Cu^+)} 1/2 GSSG + NO$	$r_{14NO} = k_{14NO} [GSNO]^2$
(15)	$CcOx + NO \Rightarrow CcOX.NO$	$r_{15NO} = k_{15NO} [CcOx][NO]$
(16)	$FeL_n + NO \Rightarrow FeL_n.NO$	$r_{16NO} = k_{16NO} [FeL_n][NO]$
(17)	$FeL_n.NO + GSH \Rightarrow GSNO + FeL_n$	$r_{17NO} = k_{17NO} [FeL_n.NO][GSH]$
(17b)	$GSH + O_2^- \Rightarrow 1/2 GSSG + \text{products}$	$r_{17bNO} = k_{17bNO} [GSH]^2 [O_2^-]^2$

Table A.10. Reaction rate constants of model 2

Index	Reactions of Model 2	Reaction Rate Constants
(1)	$0 \Rightarrow NO$	$k_{1NO} = 1000 \mu M / s$
(2)	$0 \Rightarrow O_2^-$	$k_{2NO} = 4219 \mu M / s$
(3)	$0 \Rightarrow GSH$	$k_{3NO} = 0 \mu M / s$
(4)	$NO + O_2^- \Rightarrow ONOO^-$	$k_{4NO} = 6700 \mu M^{-1} s^{-1}$
(5)	$SOD + O_2^- + Hp \Rightarrow SOD + 1/2 O_2 + 1/2 H_2 O_2$	$k_{5NO} = 2400 \mu M^{-1} s^{-1}$
(6)	$ONOO^- + GSH \Rightarrow GSNO + \text{products}$	$k_{6NO} = 84.39 \times 10^{-3} \mu M^{-1} s^{-1}$
(7)	$ONOO^- + GPX \Rightarrow GPX + \text{products}$	$k_{7NO} = 2 \mu M^{-1} s^{-1}$
(8)	$ONOO^- + CO_2 \Rightarrow \text{products}$	$k_{8NO} = 0.058 \mu M^{-1} s^{-1}$
(9)	$ONOO^- + Cc \Rightarrow Cc + \text{products}$	$k_{9NO} = 0.025 \mu M^{-1} s^{-1}$
(10)	$2GSNO + O_2^- + H_2 O \Rightarrow GSSG + \text{products}$	$k_{10NO} = 17.84 \times 10^{-6} \mu M^{-2} s^{-1}$
(11)	$N_2 O_3 + GSH \Rightarrow GSNO + \text{products}$	$k_{11NO} = 66 \mu M^{-1} s^{-1}$
(12a)	$2NO + O_2 \Rightarrow 2NO_2$	$k_{12aNO} = 0.0000006 \mu M^{-2} s^{-1}$
(13)	$N_2 O_3 + H_2 O \Rightarrow \text{products}$	$k_{13NO} = 0 s^{-1}$
(m)	$GSSG + NADPH + Hp \Rightarrow 2GSH + NADP_p$	$k_m = 6.95 s^{-1}$
(12bp)	$NO_2 + NO \Leftrightarrow N_2 O_3$	$k_{12bNOp} = 1100 \mu M^{-1} s^{-1}$
(12bm)		$k_{12bNOm} = 81000 s^{-1}$
(14)	$GSNO \xrightarrow{(Cu^+)} 1/2 GSSG + NO$	$k_{14NO} = 7.59 \times 10^{-3} \mu M^{-1} s^{-1}$
(15)	$CcOx + NO \Rightarrow CcOX.NO$	$k_{15NO} = 100 \mu M^{-1} s^{-1}$
(16)	$FeL_n + NO \Rightarrow FeL_n NO$	$k_{16NO} = 1.21 \mu M^{-1} s^{-1}$
(17)	$FeL_n NO + GSH \Rightarrow GSNO + FeL_n$	$k_{17NO} = 66 \mu M^{-1} s^{-1}$
(17b)	$GSH + O_2^- \Rightarrow 1/2 GSSG + \text{products}$	$k_{17bNO} = 0.0002 \mu M^{-1} s^{-1}$

Table A.11. Equilibrium levels and initial concentrations used in model 2

Equilibrium Concentrations
$[\text{SOD}]_{\infty} = 10 \mu\text{M}$
$[\text{O}_2]_{\infty} = 10 \mu\text{M}$
Initial Concentrations
$[\text{CcOx}]_0 = 0.1 \mu\text{M}$
$[\text{FeL}_n]_0 = 0.05 \mu\text{M}$
Unstable State
$[\text{NO}]_0 = 1200 \mu\text{M}$
$[\text{GSNO}]_0 = 500 \mu\text{M}$
$[\text{O}_2^-]_0 = 100 \mu\text{M}$
$[\text{ONOO}^-]_0 = 1100 \mu\text{M}$
Stable State
$[\text{GSH}]_0 = 10^3 \mu\text{M}$

A.2. Model 3

Table A.12. Additional reactions combining model 1 and model 2 (model 3)

Reaction Index	Reactions of Combining Model 1 and Model 2	Reaction Rate Constants
(1)	$\text{ONOO}^- + \text{MPTP}_{c1} \Rightarrow \text{MPTP}_{act} + \text{products}$	$r_{18\text{NO}} = k_{18\text{NO}}[\text{ONOO}^-][\text{MPTP}_{c1}]$
(2)	$\text{N}_2\text{O}_3 + \text{casp8} \Rightarrow \text{casp8.NO} + \text{NO}_2$	$r_{19\text{NO}} = k_{19\text{NO}}[\text{N}_2\text{O}_3][\text{casp8}]$
(3)	$\text{FeL}_n\text{NO} + \text{casp8} \Rightarrow \text{casp8.NO} + \text{FeL}_n$	$r_{20\text{NO}} = k_{20\text{NO}}[\text{FeL}_n\text{NO}][\text{casp8}]$
(4)	$\text{FeL}_n\text{NO} + \text{casp9} \Rightarrow \text{casp9.NO} + \text{FeL}_n$	$r_{21\text{NO}} = k_{21\text{NO}}[\text{FeL}_n\text{NO}][\text{casp9}]$
(5)	$\text{FeL}_n\text{NO} + \text{casp3} \Rightarrow \text{casp3.NO} + \text{FeL}_n$	$r_{22\text{NO}} = k_{22\text{NO}}[\text{FeL}_n\text{NO}][\text{casp3}]$

Table A.13. Rate constants of additional reactions combining model 1 and model 2

(model 3)

Reaction Index	Reactions of Combining Model 1 and Model 2	Reaction Rate Constants
(1)	$\text{ONOO}^- + \text{MPTP}_{c1} \Rightarrow \text{MPTP}_{act} + \text{products}$	$k_{18\text{NO}} = 1 \mu\text{M}^{-1}\text{s}^{-1}$
(2)	$\text{N}_2\text{O}_3 + \text{casp8} \Rightarrow \text{casp8.NO} + \text{NO}_2$	$k_{19\text{NO}} = 10 \mu\text{M}^{-1}\text{s}^{-1}$
(3)	$\text{FeL}_n\text{NO} + \text{casp8} \Rightarrow \text{casp8.NO} + \text{FeL}_n$	$k_{20\text{NO}} = 66 \mu\text{M}^{-1}\text{s}^{-1}$
(4)	$\text{FeL}_n\text{NO} + \text{casp9} \Rightarrow \text{casp9.NO} + \text{FeL}_n$	$k_{21\text{NO}} = 66 \mu\text{M}^{-1}\text{s}^{-1}$
(5)	$\text{FeL}_n\text{NO} + \text{casp3} \Rightarrow \text{casp3.NO} + \text{FeL}_n$	$k_{22\text{NO}} = 66 \mu\text{M}^{-1}\text{s}^{-1}$

APPENDIX B: DETERMINATION OF CASPASE-3 THRESHOLD VALUE

The radius of the cell is assumed to be 10 micrometer. For the spherical cell geometry, following formula gives the volume of the cell:

$$V = \frac{4}{3}\pi R^3 = \frac{4}{3}\pi(10^{-5})^3 = 4.187 \times 10^{-15} m^3 = 4.187 \times 10^{-12} L \quad (\text{B.1})$$

Now, to calculate the threshold concentration of caspase-3 protein for the onset of apoptosis let

$$M = \frac{n}{V} \quad (\text{B.2})$$

where M is the concentration in terms of (mol/L), n is the number of moles of caspase-3, V is the volume of the cell

If the necessary number of caspase-3 molecules for the onset of apoptosis is assumed to be 2500 molecules (N), then

$$n = \frac{N}{\text{Avagadro Number}} = \frac{2500}{6.023 \times 10^{23}} = 4.151 \times 10^{-21} \text{ mol} \quad (\text{B.3})$$

$$M_{\text{casp3}} = \frac{4.151 \times 10^{-21} \text{ mol}}{4.187 \times 10^{-12} L} = 9.91 \times 10^{-10} M = 0.991 \text{ nM} \approx 1 \text{ nM} \quad (\text{B.4})$$

REFERENCES

- Alberts, B., A. Johnson, J. Lewis, M. Raff, K. Roberts, and P. Walter, 2002, "Molecular Biology of the Cell", *Garland Science*, 4th Edition, pp. 1010-1026.
- Bagci, E.Z., Y. Vodovotz, T. Billiar, B. Ermentrout, and I. Bahar, 2006, "Bistability in Apoptosis: Roles of Bax, Bcl-2, and Mitochondrial Permeability Transition Pores", *Biophysical Journal*, Vol. 90, Issue 5, pp. 1546–1559.
- Bagci, E.Z., Y. Vodovotz, T. Billiar, B. Ermentrout, and I. Bahar, 2008 "Computational Insights on the Competing Effects of Nitric Oxide in Regulating Apoptosis", *Public Library of Science Journal*, Vol. 3, Issue 5, pp. e2249.
- Beere, H.M., B.B. Wolf, K. Cain, D.D. Mosser, A. Mahboubi, T. Kuwana, P. Taylor, R.I. Morimoto, G.M. Cohen, and D. R. Green, 2000, "Heat-Shock Protein 70 Inhibits Apoptosis by Preventing Recruitment of Procaspase-9 to the Apaf-1 Apoptosome", *Nature Cell Biology*, Vol. 2, pp. 469 - 475.
- Bentele, M., I. Lavrik, M. Ulrich, S. Stosser, D.W. Heermann, H. Kalthoff, P.H. Kramer, and R. Eils, 2004, "Mathematical Modeling Reveals Threshold Mechanism in CD95-Induced Apoptosis", *J. Cell Biol.*, Vol. 166, pp. 839-851.
- Curtin, J.F., and T.G. Cotter, 2003, "Live and Let Die: Regulatory Mechanisms in FAS-Mediated Apoptosis", *Cellular Signalling*, Vol. 15, pp. 983-992.

- Dash, P.R., J.E. Cartwright, and G.S. Whitley, 2003, "Nitric Oxide Inhibits Polyamine-Induced Apoptosis in the Human Extravillous Trophoblast Cell Line SGHPL-4", *Hum. Reprod.*, Vol. 18, pp. 959-968.
- Eissing, T., H. Conzelmann, E.D. Gilles, F. Allgöwer, E. Bullinger, and P. Scheurich, 2004, "Bistability Analyses of a Caspase-Activation Model for Receptor-Induced Apoptosis", *The Journal of Biological Chemistry*, Vol. 279, Issue 35, pp. 36892-36897.
- Ellison, P., and M. Feinberg, 2000, "How Catalytic Mechanisms Reveal Themselves in Multiple Steady-State Data: I. Basic Principles", *Journal of Molecular Catalysis A: Chemical*, Vol. 154, pp. 155-167.
- Ermentrout, B., 2002, "Simulating, Analyzing, and Animating Dynamical Systems: A Guide to XPPAUT for Researchers and Students", *SIAM*, PA, USA.
- Feinberg, M., 1977, "Mathematical Aspects of Mass-Action Kinetics", Ch.1 in *Chemical Reaction Theory: A Review* (eds. N. Amundson and L. Lapidus), *Prentice-Hall*, Englewood Cliffs.
- Feinberg, M., 1979, "Lectures on Chemical Reaction Networks", *Notes of Lectures Given at the Mathematics Research Centre*, University of Wisconsin.
- Feinberg, M., 1987, "Chemical Reaction Network Structure and the Stability of Complex Isothermal Reactors I. The Deficiency Zero and Deficiency One Theorems", *Chemical Engineering Science*, Vol. 42, pp. 2229-68.

Feinberg, M., 1988, "Chemical Reaction Network Structure and the Stability of Complex Isothermal Reactors II. Multiple Steady States for Networks of Deficiency One", *Chemical Engineering Science*, Vol. 43, pp. 1-25.

Feinberg, M., 1995, "Multiple Steady States for Chemical Reaction Networks of Deficiency One", *Archive for Rational Mechanics and Analysis*, Vol. 132 pp. 371-406.

Ferrell, J.E., Jr, and W. Xiong, 2001, "Bistability in Cell Signaling: How to Make Continuous Processes Discontinuous, and Reversible Processes Irreversible", *Chaos*, Vol. 11, pp. 227-236.

Ferrell, J.E. Jr., 2002, "Self-Perpetuating States in Signal Transduction: Positive Feedback, Double-Negative Feedback and Bistability", *Current Opinion in Cell Biology*, Vol. 14(2), pp. 140-148.

Fussenegger, M., J.E. Bailey, and J. Varner, 2000, "A Mathematical Model of Caspase Function in Apoptosis", *Nature Biotech.*, Vol. 18, pp. 768-774.

Garrido, C., E. Schmitt, C. Candé, N. Vahsen, A. Parcellier, and G. Kroemer, 2003, "HSP27 and HSP70: Potentially Oncogenic Apoptosis Inhibitors", *Cell Cycle*, Vol. 2, pp. 579-584.

Hu, T.M., W.L. Hayton, and S.R. Mallery, 2006, "Kinetic Modeling of Nitric-Oxide Associated Reaction Network", *Pharmaceutical Research*, Vol. 23, pp. 1702–1711.

Kim, P.K.M., R. Zamora, P. Petrosko, and T.R. Billiar, 2001, "The Regulatory Role of Nitric Oxide in Apoptosis", *Int Immunopharmacol*, Vol. 1, pp. 1421–1441.

- Lavrik, I.N., A. Golks, D. Riess, M. Bentele, R. Eils, and P. H. Krammer, 2007, "Analysis of CD95 Threshold Signaling: Triggering of CD95 (FAS/APO-1) at Low Concentrations Primarily Results In Survival Signaling", *J. Biol. Chem.*, Vol. 282, pp. 13664-13671.
- Legewie, S., N. Blüthgen, and H. Herzel, 2006, "Mathematical Modeling Identifies Inhibitors of Apoptosis as Mediators of Positive Feedback and Bistability", *PLoS. Comput. Biol.*, Vol. 2, pp. e120.
- Loughran, P.A., E.Z. Bagci, R. Zamora, Y. Vodovotz, and T.R. Billiar, 2009, "The Role of Nitric Oxide in Apoptosis and Autophagy: Biochemical and Computational Studies", *Nitric Oxide*, Ed. L. Ignarro.
- Nakabayashi, J, and A. Sasaki, 2006, "A Mathematical Model for Apoptosome Assembly: The Optimal Cytochrome C/Apaf-1 Ratio", *J Theor Biol*, Vol. 242, pp. 280–287.
- Newton, K, and A. Strasser, 2003, "Caspases Signal Not Only Apoptosis But Also Antigen-Induced Activation in Cells of the Immune System", *Genes Dev.*, Vol. 17, pp. 819-825.
- Özören, N. and W.S. El-Deiry, 2002, "Defining Characteristics of Types I and II Apoptotic Cells in Response to TRAIL", *Neoplasia*, Vol. 4, pp. 551-557.
- Packham, G., and F.K. Stevenson, 2005, "Bodyguards and Assassins: Bcl-2 Family Proteins and Apoptosis Control in Chronic Lymphocytic Leukaemia", *Immunology*, Vol. 114, pp. 441–449.

- Ryu, S., S. Lin, N. Ugel, M. Antonioti, and B. Mishra, 2009, "Mathematical Modeling of the Formation of Apoptosome In Intrinsic Pathway of Apoptosis", *Systems and Synthetic Biology*, Vol. 2, pp. 49-66.
- Saez-Rodriguez, J., A. Hammerle-Fickinger, O. Dalal, S. Klamt, E.D. Gilles, and C. Conradi, 2008, "Multistability of Signal Transduction Motifs", *IET Systems Biology*, Vol. 2, pp. 80-93.
- Siehs, C., R. Oberbauer, G. Mayer, A. Lukas, and B. Mayer, 2002, "Discrete Simulation of Regulatory Homo- and Heterodimerization in the Apoptosis Effector Phase", *Bioinformatics*, Vol. 18, pp. 67-76.
- Stennicke, H. R., and G.S. Salvesen, 1999, "Catalytic Properties of the Caspases", *Cell Death and Differentiation*, Vol. 6, pp. 1054–1059.
- Stucki, J.W., and H.U. Simon, 2005, "Mathematical Modeling of Caspase-3 Activation and Degradation", *J. Theoretical Biol.*, Vol. 234, pp. 123-131.
- Tyson, J.J., K.C. Chen, and B. Novak, 2003, "Sniffers, Buzzers, Toggles and Blinkers: Dynamics of Regulatory and Signaling Pathways in the Cell", *Current Opinion in Cell Biology*, Vol. 15, pp. 221-231.
- Xiong, W., and J.E., Jr. Ferrell, 2003, "A Positive-Feedback-Based Bistable 'Memory Module' that Governs a Cell Fate Decision", *Nature*, Vol. 426 (6965), pp. 460-465.
- Zou, H., Y. Li, X. Lui, and X. Wang, 1999, "An Apaf-1.Cytochrome C Multimeric Complex is a Functional Apoptosome that Activates Caspase-9", *J. Biol. Chem.*, Vol. 274 (17), pp. 11549-11556.